https://doi.org/10.5194/acp-2022-598
Preprint. Discussion started: 29 August 2022

Atmospheric Chemistry and Physics Discussions

The importance of acid processed meteoric smoke relative to meteoric fragments for crystal nucleation in polar stratospheric clouds

Alexander D. James[1], Finn Pace[1], Sebastien N. F. Sikora[2], Graham W. Mann[2], John M. C. Plane[1], Benjamin J. Murray[2]

[1]School of Chemistry, University of Leeds, Leeds, LS9 2JT, UK
[2]School of Earth and Environment, University of Leeds, LS9 2JT, UK

Correspondence to: Alexander D. James (A.James1@leeds.ac.uk) and Benjamin J. Murray (B.J.Murray@leeds.ac.uk)

Abstract. Nitric Acid Trihydrate (NAT) crystal formation in the absence of water ice is important for a subset of Polar Stratospheric Clouds (PSCs) and thereby ozone depletion. It has been suggested that either fragmented meteoroids or meteoric smoke particles (MSPs), or possibly both, are important as heterogeneous nuclei of these crystals. Previous work has focused on the nucleating ability of meteoric material in nitric acid in the absence of sulfuric acid. However, it is known that when immersed in stratospheric sulfuric acid droplets, metal-containing meteoric material particles partially dissolve and components can re-precipitate as silica and alumina that have different morphologies to the original meteoric material. Hence, in this study we experimentally and theoretically explore the relative role that sulfuric acid-processed meteoric smoke and meteoric fragments may play in NAT nucleation in PSCs.

We compared meteoric fragments that had been recently prepared (by milling a meteorite sample) to a sample annealed under conditions designed to simulate heating during entry into the Earth's atmosphere. Whilst the addition of sulfuric acid decreased the nucleating ability of the recently milled meteoric material relative to nucleation in binary nitric acid-water solutions (at similar NAT saturation ratio), the annealed meteoric fragments nucleated NAT with a similar effectiveness in both solutions. However, combining our results with measured fluxes of meteoric material to the Earth, sedimentation modelling and recent experiments on fragmentation of incoming meteoroids, suggests that there are unlikely to be sufficient fragments to contribute to the nucleation of crystalline NAT particles.

We then considered silica formed from sulfuric acid processed meteoric smoke particles. Our previous work showed that nano-particulate silica (radius ~6 nm) is a relatively poor promoter of nucleation compared with micron scaled silica particles, which were more effective. Both materials have similar chemical and structural (crystallographically amorphous) properties, indicating size is critical. Here we account for surface curvature of primary grains using Classical Nucleation Theory (CNT) to explore this size dependence. This model is able to explain the discrepancy in nucleation effectiveness of fumed silica and fused quartz, by treating their nucleating activity (contact angle) as equal but with differing particle size (or surface curvature), assuming interfacial energies that are physically reasonable. Here we use this CNT model to present evidence that nucleation

https://doi.org/10.5194/acp-2022-598
Preprint. Discussion started: 29 August 2022


Atmospheric Chemistry and Physics Discussions

of NAT on acid processed MSPs, where the primary grain size is 10s nm, is also effective enough to contribute to NAT crystals in early season PSCs where there is an absence of ice.

This study demonstrates that modelling of crystal nucleation in PSCs and resulting ozone depletion relies on accurate understanding of the transport and chemical processing of MSPs. This will affect estimated sensitivity of stratospheric chemistry to rare events such as large volcanic eruptions and long-term forecasting of ozone recovery in a changing climate.

1 Introduction

With record ozone loss observed in the Arctic winter 2019-2020 (Lawrence et al., 2020), it is increasingly clear that understanding the chemistry which occurs in the winter polar vortex is important for predicting future recovery of polar ozone. Aerosol science, and nucleation of crystalline components of Polar Stratospheric Clouds (PSCs) in particular, remains a key uncertainty in modelling chlorine and bromine activation and ozone destruction. Nucleation is particularly important because the crystallisation of nitric acid hydrates and water ice affects both the total amount and the kinetics of ozone destroying species activation of the heterogeneous surface of PSC particles (Brakebusch et al., 2013). The growth and sedimentation of these nitric acid particles then also leads to denitrification, which slows the deactivation of active species (Wegner et al., 2012).

In many clouds NAT is thought to nucleate on ice crystals, but it has been shown that crystalline nitric acid particles can sometimes form in conditions where ice is not thermodynamically stable (Mann et al., 2005;Tritscher et al., 2021), though in some winters effectively all cloud could contain water ice (Carslaw et al., 1999). Current models of crystal formation involve heterogeneous nucleation of water ice and nitric acid trihydrate (NAT) (Hoyle et al., 2013;Engel et al., 2013;James et al., 2018;Steiner et al., 2021). Nitric acid dihydrate (NAD) may also form, though this is not currently considered in atmospheric models (Grothe et al., 2008). Whilst meteoric material is assumed to be the heterogeneous nucleus, terrestrial aerosol is also present in the stratosphere, also entrained in sulfuric acid droplets, but has been considered unlikely to contribute to nucleation in PSC as this tends to occur in descending airmasses originating from the mesosphere (Kremser et al., 2016). Global models do not yet include a parameterisation of this activity based on laboratory measurements of reasonable heterogeneous nucleator surfaces, but rather have been tuned to observed NAT particle concentrations (Grooß et al., 2014;Voigt et al., 2005). However, models which are not constrained by a physical understanding, tested in laboratory experiments, may have a limited capacity for predicting future trends in ozone depletion.

Figure X1 shows possible pathways for meteoric material through the atmosphere, starting from various populations of incoming interplanetary dust. On heating by atmospheric friction the first processes that may occur are fragmentation or ablation of the incoming meteoroid (Carrillo-Sánchez et al., 2020;Subasinghe et al., 2016). Unablated meteoroids, partially melted cosmic spherules and meteoric fragments gravitationally sediment according to their size, whilst ablated metal atoms are oxidized to form a variety of species (oxides, hydroxides and carbonates) that then polymerise to form Meteoric Smoke

https://doi.org/10.5194/acp-2022-598
Preprint. Discussion started: 29 August 2022


Atmospheric Chemistry and Physics Discussions

Particles (MSPs) (Plane et al., 2015). MSPs are generally small enough that they do not gravitationally sediment at significant speeds, rather they are carried by the atmospheric circulation, with atmospheric lifetimes on the order of several years (Brooke et al., 2017;Dhomse et al., 2013). As MSPs and fragments descend through the atmosphere, gas-phase species can be taken up on their surfaces (Frankland et al., 2015;James et al., 2017;Saunders et al., 2012). It has been shown that meteoric smoke will become entrained within sulfuric acid droplets in the Junge layer (Brooke et al., 2017), and partially dissolve (Murphy et al., 2014;Bogdan et al., 2003), but the effect on meteoric fragments has not been previously considered.

https://doi.org/10.5194/acp-2022-598
Preprint. Discussion started: 29 August 2022

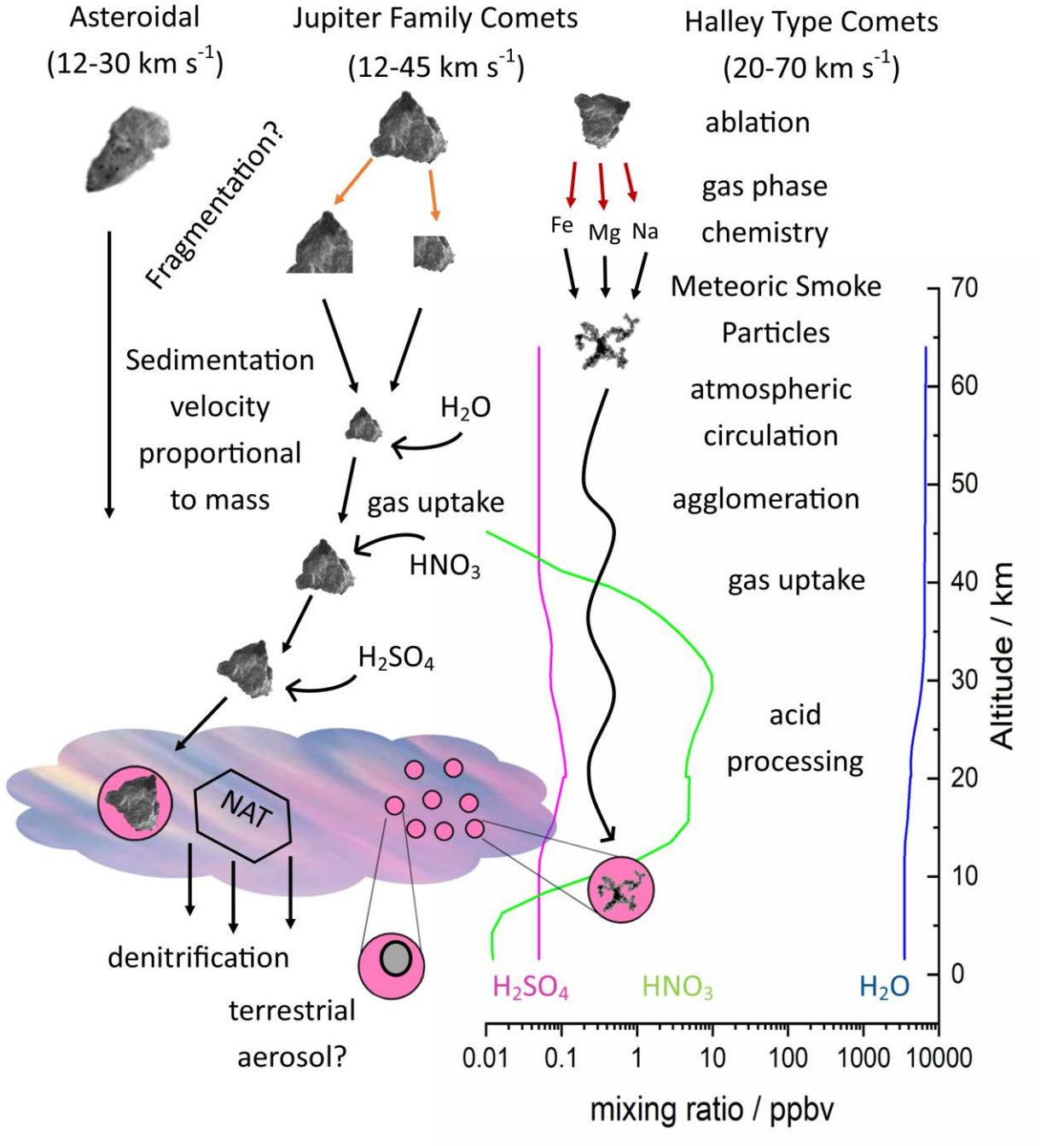

Figure 1: Possible pathways (black arrows) for meteoric material through the atmosphere. Brackets show the limits of entry velocity. Types of aerosol and processes affecting them are shown. Altitudes and concentrations are indicative of approximately where each process is important. See text for detailed explanation.

https://doi.org/10.5194/acp-2022-598
Preprint. Discussion started: 29 August 2022


Atmospheric Chemistry and Physics Discussions

Heterogeneous nucleation can be controlled either by relatively rare active sites, or by a surface of relatively uniform activity (Murray et al., 2012). In either case, a solid nucleating particle (NP) included in the supercooled liquid droplet facilitates nucleation of the crystal (here we use "solid" to refer to the nucleating particle and "crystal" to the newly forming phase). With a rare active site, the activity of the NP is parameterised by the number of sites per unit area that cause nucleation under a specific set of conditions. In our previous work we used this method to parameterise the activity of a variety of analogues for meteoric material and compare them to an observed cloud (James et al., 2018). In previous modelling of PSC nucleation (Hoyle et al., 2013), it had been assumed that meteoric material causes heterogeneous nucleation kinetically at a rate determined by a distribution of active sites according to the Classical Nucleation Theory (CNT). In CNT a rate of nucleation is calculated based on the system's ability to overcome barriers to diffusion to the interface between the liquid and the cluster of nucleating crystal, ΔF, and to formation of the crystalline molecular cluster of critical size, above which the crystalline phase grows freely, ΔG^*. This rate, J_{het}, is defined as equation E1 (Pruppacher and Klett, 1978;Murray et al., 2012).

$$J_{het}/cm^{-2}s^{-1} = \frac{n_{mol}k_BT}{h} e^{-\Delta F/k_BT} e^{-\Delta G^* f_{het}/k_BT} \quad \text{(E1)}$$

where n_{mol} is the number of molecules per unit volume in the liquid and k_B and h are the Boltzmann and Planck constants, respectively. The geometric factor, f_{het}, can be conceptualised as the relative reduction in the crystalline cluster volume required for critical size. Most generally, it is defined by E2.

$$f_{het} = \frac{1}{2}\left(1 + \left(\frac{1-mX}{\varphi}\right)^3 + X^3\left(2 - \left(\frac{3(X-m)}{\varphi}\right) + \left(\frac{(X-m)}{\varphi}\right)^3\right) + 3mX^2\left(\frac{(X-m)}{\varphi} - 1\right)\right) \quad \text{(E2)}$$

where $X = \frac{r_{NP}}{r^*}$ is the ratio between the radius of the nucleating particle, r_{NP}, and the critical cluster, r^*, the contact parameter $m = \cos\theta$ where θ is the contact angle, and $\varphi = \sqrt{(1 + X^2 - 2Xm)}$. The radius of the critical cluster size can be determined from thermodynamic properties of the system by E3.

$$r^* = \frac{2V_{mol}^2\sigma}{(k_BT\ln(S))^2} \quad \text{(E3)}$$

where V_{mol} is the volume of one molecule of solid composition, S is the saturation ratio (the ratio of free energies of the supercooled liquid to the system at thermodynamic equilibrium), and σ is the interfacial energy between the crystal and liquid. ΔG^* can similarly be determined from thermodynamic properties:

$$\Delta G^* = \frac{16\pi}{3}\frac{V_{mol}^2\sigma^3}{(k_BT\ln(S))^2} \quad \text{(E4)}$$

Following nucleation the crystalline phase will grow at the expense of the liquid droplet, and since the vapour pressure over the solid phase is lower than that over the liquid phase, the composition of other droplets can also be affected (Carslaw et al., 2002). The result can be a cloud where relatively few crystals form, grow rapidly and sediment until they reach a region warm

https://doi.org/10.5194/acp-2022-598
Preprint. Discussion started: 29 August 2022


Atmospheric Chemistry and Physics Discussions

enough for the particles to evaporate (Voigt et al., 2005), causing a vertical redistribution of NO_y, including nitric acid (Fueglistaler et al., 2002). This so-called denitrification can lead to enhanced ozone depletion because a reduction of NO_y species slows deactivation of Cl and Br catalytic ozone destroyers. Ozone depletion is therefore sensitive to the nucleation of crystalline PSCs, both through the available catalytic aerosol surface and through the denitrification process (Wegner et al., 2012).

The activity of some heterogeneously nucleating materials has been found in the past to be affected by the presence in solution of, or pre-treatment by, acids or other solutes (Whale et al., 2018;Wex et al., 2014). In particular H_2SO_4 has been found to deactivate many ice nucleating materials, even where some other acids had little effect (Kumar et al., 2019;Fahy et al., 2022). To date no systematic test has been made on the effect of H_2SO_4 on heterogeneous nucleation in PSCs, although there is H_2SO_4 present in the liquid stratospheric aerosol from which crystalline PSC particles form (Carslaw et al., 1997).

In this study we assess the potential pathways to the heterogeneous nucleation of NAT through nucleation on meteoric fragments and nucleation on meteoric smoke. In the first part of the paper we experimentally explore the sensitivity of the nucleation activity of meteoric fragments to H_2SO_4 and the heating that occurs on entry to the atmosphere. We then use sedimentation modelling and comparison to measurements of meteoric input to the Earth to assess the likelihood that meteoric fragments contribute to crystal nucleation in PSCs and constrain their flux. In the second part we theoretically assess whether nucleation on silica particles resulting from acid processing of MSPs might contribute to the NAT population. In the past it has been shown that silica can nucleate nitric acid hydrates, but its activity varies massively (James et al. 2018; Bogdan et al., 2003), with smaller silica particles nucleating NAT less effectively. We develop a size dependent nucleation parameterisation for nucleation of NAT on silica, constrained by our previous experimental results, to assess the likelihood that acid processed MSPs contribute to crystal nucleation in PSCs. We investigate specifically whether nucleation activity of these heterogeneous materials is sufficient to explain observed cloud crystal number concentrations in the absence of water ice.

2 Methods

To determine the heterogeneous activity of analogues for meteoric material, arrays of 1 µl droplets were cooled until they crystallised and the nucleation events observed using a liquid nitrogen-cooled cold stage shown in Figure 2 a, described previously (Holden et al., 2019). Nucleation, crystal growth and melting were observed using a CMEX-5 pro CCD camera (Figure 2 b-f). Temperature was measured using a platinum resistance thermometer and controlled by balancing a constant liquid nitrogen cryogen flow with resistive heating cartridges embedded in the aluminium cold stage. Droplet arrays were pipetted onto a hydrophobic glass slide, sealed into a cell by surrounding with a viton O-ring used as a spacer and covered with a second glass slide, then a dry nitrogen flow was used to prevent icing of the upper surface of the glass slide during cooling. Reflected illumination was provided by four plane polarised LEDs.

https://doi.org/10.5194/acp-2022-598
Preprint. Discussion started: 29 August 2022

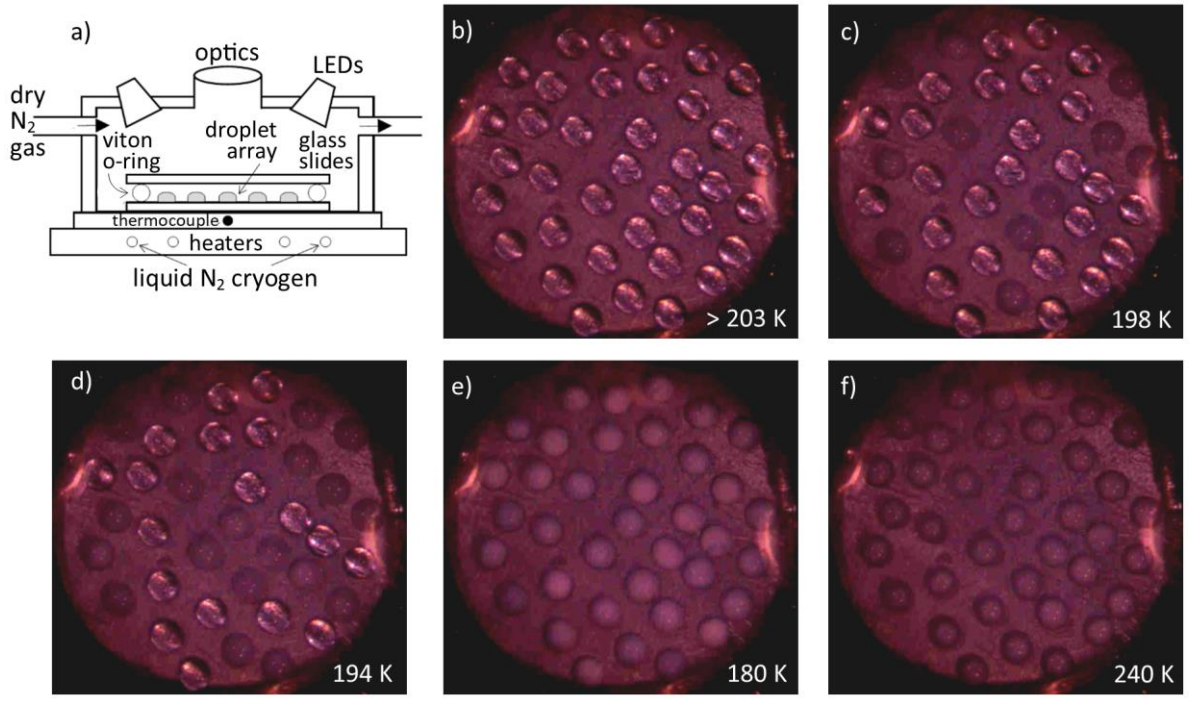

Figure 2: a) Diagram showing experimental apparatus. An aluminium stage is cooled by a constant flow of liquid nitrogen and temperature and rate of change is controlled by heating cartridges embedded in the aluminium. A hydrophobic glass slide is placed on this surface, an array of 1 µl droplets is pipetted onto the slide, surrounded by a greased viton o-ring and covered with a second slide to minimise concentration change by mass transfer between liquid and vapour. A dry nitrogen flow is passed over this sealed cell to prevent ice deposition from the atmosphere at low temperature. The cell is lit using plane polarised LEDs and reflected light images recorded with a microscope equipped with a CCD camera. b-e) droplet arrays showing nucleation and crystal growth on cooling, f) partially melted array on warming.

An analogue for meteoric fragments was produced by grinding a sample of the Allende meteorite (Clarke et al., 1971) with a pestle and mortar until it passed through an 18 µm diameter sieve (Endecotts test sieves), referred to as 'recently ground' to distinguish from samples held (to these experiments performed in 2020) since our previous work in 2016 (James et al., 2018). Some of this recently ground material was further treated to simulate frictional heating during atmospheric entry which leads to meteor fragmentation by annealing (heating) under an N_2 atmosphere. Temperature was ramped at 16 K min^{-1} to 700 K in a tube furnace (Carbolite Gero) and held for half an hour. Under this heating regime, essentially all the refractory organic material in the ground meteorite pyrolyzes (Bones et al., 2022). This Annealed Allende (AA) sample was stored in a desiccator before samples were removed to make up droplet suspensions. Aqueous acid 'control' solutions and suspensions of heterogeneous material were prepared by mass dilution from 69 wt% HNO_3 (Aristar, trace analysis grade), and 95 wt% H_2SO_4 (Acros organics, 96 %, other H_2SO_4 suppliers and grades were tested but found to have higher nucleation temperatures in control experiments without added heterogeneous material i.e. higher levels of nucleation active contamination). Suspensions

https://doi.org/10.5194/acp-2022-598
Preprint. Discussion started: 29 August 2022


Atmospheric Chemistry and Physics Discussions

were made up by first preparing the acid solution in a cold sonic bath (20 % aqueous propylene glycol cooled with CO_2 cardice to below 273 K, ranging down to 250 K), then adding the appropriate amount of meteoritic fragment analogue and sonicating for 10 minutes. Solutions were cooled to limit the possible chemical alteration of the heterogeneous nucleating material by acid solution, which might be faster at room temperature than under stratospheric conditions. Suspensions were stored in the cold bath and a new array of droplets tested at approximately hourly intervals to check for any time dependence of acid sensitivity.

Droplet arrays containing a range of Allende meteorite concentrations were prepared, either with or without 0.5 wt% H_2SO_4. This H_2SO_4 concentration was chosen as it is similar to the lowest at thermodynamic equilibrium at temperatures where nitric acid hydrates might form in the absence of water ice (Carslaw et al., 1997). In some cases the HNO_3 concentration was varied from 40 up to 43 wt%. This reduces the H_2O ice melting point by up to 20 K, leading to a greater proportion of the nucleation occurring above the ice melting point and less ambiguity in the phase which initially nucleates (Clegg et al., 1998). A full list of samples tested is shown alongside a summary of the results in Table 1 (see Section 3, below).

Ternary solutions containing fumed silica were also tested, and found to have nucleation temperatures below the instrument background, however at room temperature these suspensions were found to form a gel within several hours. Given the temperature (>250 K) at which the suspensions were made up, which may allow gel formation through increased dissolution at the particle surface, this suggests that gel formation may be an artefact of our laboratory conditions and not be important in the atmosphere. Hence, gel formation precludes experiments on fumed silica in solutions containing sulfuric acid.

Arrays of droplets were pipetted at 283 K, above the dewpoint in the room but again minimising the temperature, covered and cooled at 5 K min^{-1} to 210 K, then 1 K min^{-1} until all droplets were frozen or to a minimum temperature of 150 K. This is approximately the glass temperature of HNO_3 aqueous solutions, so further crystallisation below this temperature is unlikely (Frey et al., 2013). In several cases adjacent droplets coalesced either due to vibrations or during crystal growth, these events were discarded from the data set. Samples were then warmed at 5 K min^{-1} to 283 K, with the melting points recorded. Observed melting began at 231 ± 1 K, corresponding to the NAT / H_2O ice eutectic temperature and ended at temperatures within 1 K of the NAT melting point (S_{NAT} = 1.01 ± 0.08) for the solution concentration applied (Clegg et al., 1998). This gives confidence that the temperature control is robust and that solution concentrations do not significantly change across the experiment. In a few control experiments changes in brightness occurred on warming between 205 (the NAD / H_2O ice eutectic) and 230 K. These could be indications of metastable phases either melting or recrystallizing to stable phases that are not represented in the currently accepted H_2O / HNO_3 phase diagram. We did not investigate this further since the primary goal was to quantify nucleation of crystalline phases.

https://doi.org/10.5194/acp-2022-598
Preprint. Discussion started: 29 August 2022


Atmospheric Chemistry and Physics Discussions

3 Effect of H_2SO_4 and heating on nucleation activity of meteoric fragments

Observed fraction frozen data are shown in Figure 3, for samples with and without sulfuric acid. Control experiments of binary H_2O / HNO_3 solutions are in good agreement or show a lower nucleation temperature when compared with our previous experiments using a Stirling engine cold stage (James et al., 2018). We note that the heterogeneous nucleation temperatures for one sample decreased with the time meteoric particles were suspended in HNO_3 at temperatures from 250-270 K prior to the freezing assay, gradually falling to the baseline in approximately four hours, while others did not. Addition of H_2SO_4 increases the background nucleation temperature by up to 10 K and decreases the heterogeneous nucleation temperatures for most samples. A notable exception is the annealed Allende sample, where at least the most active third of droplets nucleate significantly above the baseline in all repeat experiments.

The increased nucleation temperatures observed in control experiments with addition of H_2SO_4 are most likely due to impurities in the H_2SO_4. Wise et al. (2003) observed a similar temperature increase on addition of metal salts to H_2SO_4 solutions; however, we did not observe a similar effect in binary HNO_3 / H_2O solution (James et al., 2018). Since we tried several H_2SO_4 brands and grades and found a variable increase in nucleation temperature, we consider it unlikely that the increased crystallisation temperature on addition of metal salts is likely to occur in the atmosphere. Nucleation on heterogeneous impurities is also consistent with the variability in the background nucleation temperatures, which is significantly greater for experiments containing H_2SO_4 than those with only H_2O and HNO_3.

https://doi.org/10.5194/acp-2022-598
Preprint. Discussion started: 29 August 2022

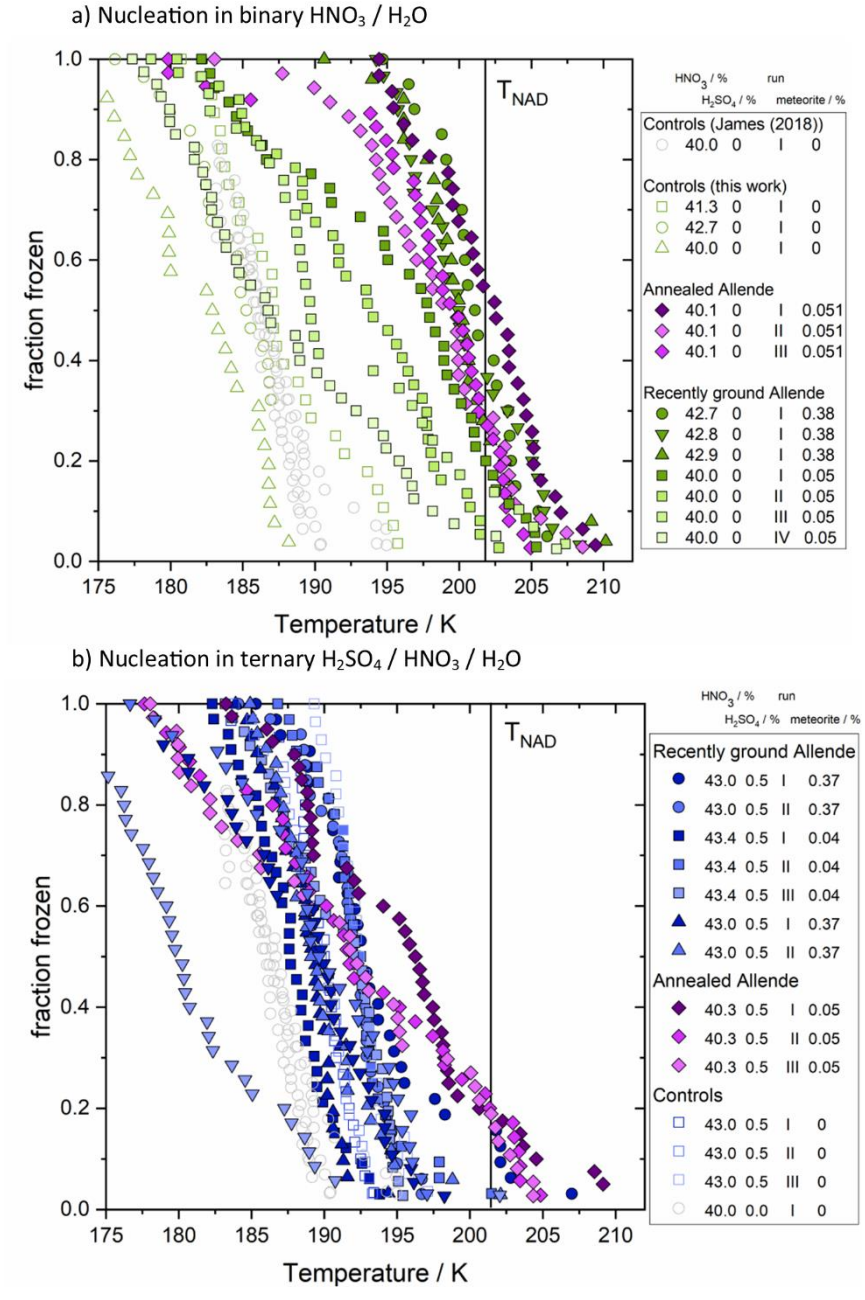

Figure 3: Fraction frozen results for meteoric fragment analogues. a) binary solution and b) ternary. Symbol shape varies for each experiment and shading for repeats, which were at intervals of approximately one hour with the sample suspension stored at <270 K in between. Open symbols show control experiments, grey open circles are data from (James et al., 2018). Legend shows the concentration of acid species and nucleating particles, and the repeat status for each data set. The melting temperature of NAD in a 40 wt% HNO_3 solution is indicated by a vertical line. The data are summarised in Table 1.

https://doi.org/10.5194/acp-2022-598
Preprint. Discussion started: 29 August 2022

Atmospheric Chemistry and Physics Discussions

Table 1: Summary of samples prepared (see Methods section) and observed heterogeneous activity

	H_2O / HNO_3 = 60/40	$H_2O/HNO_3/H_2SO_4$ = 59.5/40/0.5
Control (no added meteoric material analogue)	Nucleation temperatures agree with James et al. (2018).	Nucleation warmer and more variable than binary solutions.
Allende sample from James et al. (2018)	Nucleation temperatures agree with James et al. (2018).	Nucleation cooler than binary solutions, within baseline range. *i.e.* deactivated.
Recently ground Allende	Initially active but loses activity in HNO_3 over several hours of immersion in HNO3 solution at 250-270 K.	Deactivated.
Annealed Allende	Slightly more active than other meteoric fragment analogues either here or in James et al. (2018).	Activity above baseline and in good agreement with (James et al., 2018) in 40-60 % of droplets, resistant to acid over several hours.
Annealed Allende stored in a desiccator for one week	Deactivated	Deactivated

Even focussing on debris from a single meteorite fall, significant variability in heterogeneous nucleation behaviour is observed between very similarly treated samples. This is reasonable given the known heterogeneity of meteorite minerology. Such heterogeneity is also thought to be present in micrometeorites (Taylor et al., 2012). Annealing to simulate atmospheric entry and fragmentation seems to reduce the samples' sensitivity to acid exposure, but a reduction of activity in dry room temperature air was still observed. Since atmospheric lifetime with respect to gravitational settling is related to particle size and mass, this may constrain a minimum size below which a meteoric fragment's atmospheric lifetime is long enough to permit extensive acid processing and a reduction in nucleation activity. However, the difference between conditions such as temperature, pressure and relative humidity in our laboratory experiment and the upper atmosphere is significant, so we do not recommend any quantitative constraint on the particle size that could be deactivated by acid processing.

To facilitate a comparison with our previous experiments, and determination of the atmospheric relevance of our observed nucleation efficiencies, Figure 4 presents these results as n_s, the number of active sites per unit surface area of solid inclusion active at a given saturation ratio. Here experiments containing H_2SO_4 and using the recently ground Allende meteorite are

https://doi.org/10.5194/acp-2022-598
Preprint. Discussion started: 29 August 2022

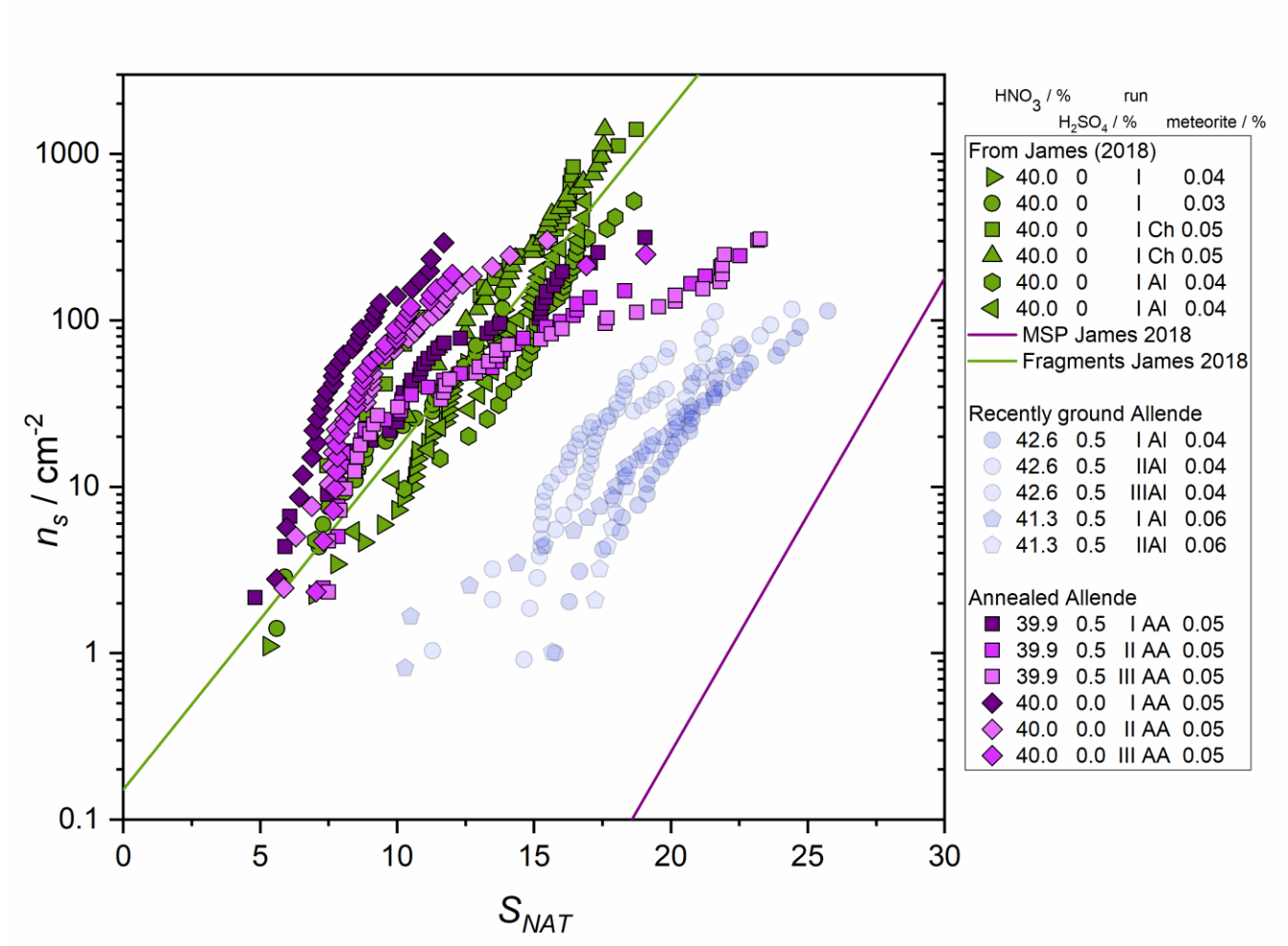

Figure 4: Nucleation effectiveness of meteoric fragment analogues with (blue) and without (green) H_2SO_4. As in James et al. (2018), unlabelled data is from experiments using the North West Africa 2502 meteorite, Ch indicates the Chergach meteorite, Al indicates Allende, see that work for details of sample preparation and experimental setup. Here AA indicates a sample of the Allende meteorite annealed to simulate relatively mild heating on atmospheric entry which could lead to fragmentation (see text for details). Green symbols with the exception of diamonds are from our previous publication. Blue data shows experiments containing H_2SO_4.

These experimental results demonstrate that, whilst acid suspension can have complex effects on the nucleating activity of fragmented meteoric material, at least some subset of the material can maintain activity, in agreement with our previous parameterisation (James et al., 2018). This allows us to carry out a more thorough evaluation of whether sufficient fragments are supplied to the lower stratosphere, with reference to the latest understanding of meteoritics and atmospheric entry. To do

https://doi.org/10.5194/acp-2022-598
Preprint. Discussion started: 29 August 2022

Atmospheric Chemistry and Physics Discussions

this, we take advantage of the linear relationship between the available surface area of nucleating particles and the final concentration of crystals. In our previous work we showed that with this parameterisation of their activity, a surface area of 0.76 $\mu m^2\ cm^{-3}$ produced around $>2 \times 10^{-5}$ NAT crystals cm^{-3}. We therefore estimate 0.2 $\mu m^2\ cm^{-3}$ as a minimum surface area that could produce the observed crystal concentration of $6 \times 10^{-6}\ cm^{-3}$.

Assuming that the mass of meteoric fragments is such that their transport is completely dominated by gravitational sedimentation, we can combine the fall speed of a given particle with constraint of the total input of meteoric material to the Earth to estimate whether this surface area might be available.

To calculate fall speed we assume a mass density of 2.2 g cm^{-3} for meteoric fragments and sedimentation velocity calculated using Stokes' law for a spherical particle falling through a stationary fluid (Jacobson, 2005). Figure 5 shows the resulting atmospheric lifetime of meteoric fragments with respect to gravitational sedimentation. For example, particles of around 0.5 µm radius or larger will fall into the stratosphere within one day. Horizontal atmospheric winds on the order of 10s m s^{-1} will move the particles on the order several km in that time, meaning that there will not be significant redistribution of fragments toward the mesospheric winter pole.

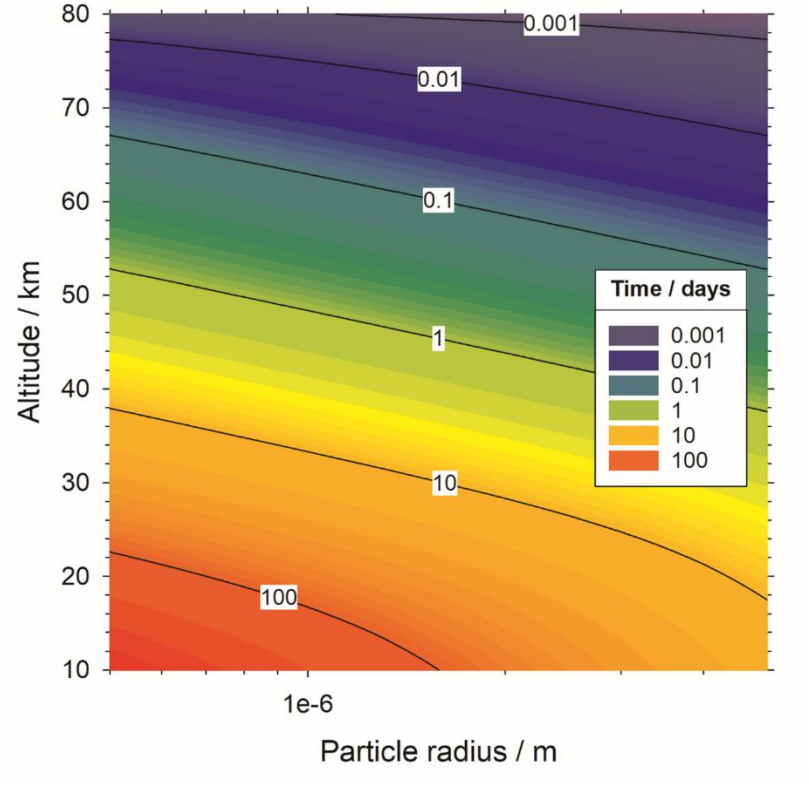

Figure 5: Cumulative time for a meteoric particle of given size to sediment gravitationally to a given altitude.

https://doi.org/10.5194/acp-2022-598
Preprint. Discussion started: 29 August 2022


Atmospheric Chemistry and Physics Discussions

We can then use known constraints of the Meteoric Input Function (MIF, ton day^{-1}) to estimate whether fragments of a given size could significantly influence nucleation in the polar stratosphere. The most recent investigations of the Earth's MIF suggest that each day 8.3 tons of meteoric material ablate and ultimately produce MSPs, 5.5 tons partially melt to produce cosmic spherules such as those observed in the South Polar Water Well (Taylor et al., 2012), and a final 14.2 tons do not heat sufficiently to melt (Carrillo-Sánchez et al., 2020). Any particles entering the Earth's atmosphere but not included in this would have to provide minimal contribution to the zodiacal scattered light, fragment to sizes smaller than 50 µm radius and provide negligible Na and Fe input to the mesosphere. Observations by aircraft in the polar stratosphere have found significant numbers of micron-size particles, with MIF estimates from 77 to 375,000 tons day^{-1} required to explain the number of particles collected (Weigel et al., 2014). Single particle mass spectrometer measurements on aircraft also detect significant numbers of meteoric particles (Schneider et al., 2021;Murphy et al., 2021;Adachi et al., 2022), and are able to investigate their composition and atmospheric distribution, but since the sulfate components are also present in stratospheric aerosol in variable amounts it is not trivial to derive MIF information from these measurements. A reasonable upper limit to the MIF comes from the Long Duration Exposure Facility (LDEF), which measured pits on surfaces exposed in near-Earth orbit and an assumed velocity of incoming particles to estimate a mass flux of 110 ± 55 ton day^{-1} (Love and Brownlee, 1993). Accounting for the mass required to explain ablated metals measured in the atmosphere and particles present in the south polar water well collections, we derive an upper limit for the mass of incoming material which could fragment at 137 ton day^{-1}.

Assuming for simplicity that this incoming mass fragments to a monodisperse particle size and is transported only by sedimentation we can calculate a resulting surface area density at PSC altitudes. This is shown in Figure 6. The implication is that all of the incoming particles would have to fragment to radii of <100 µm to provide a significant contribution to observed crystalline PSC.

https://doi.org/10.5194/acp-2022-598
Preprint. Discussion started: 29 August 2022

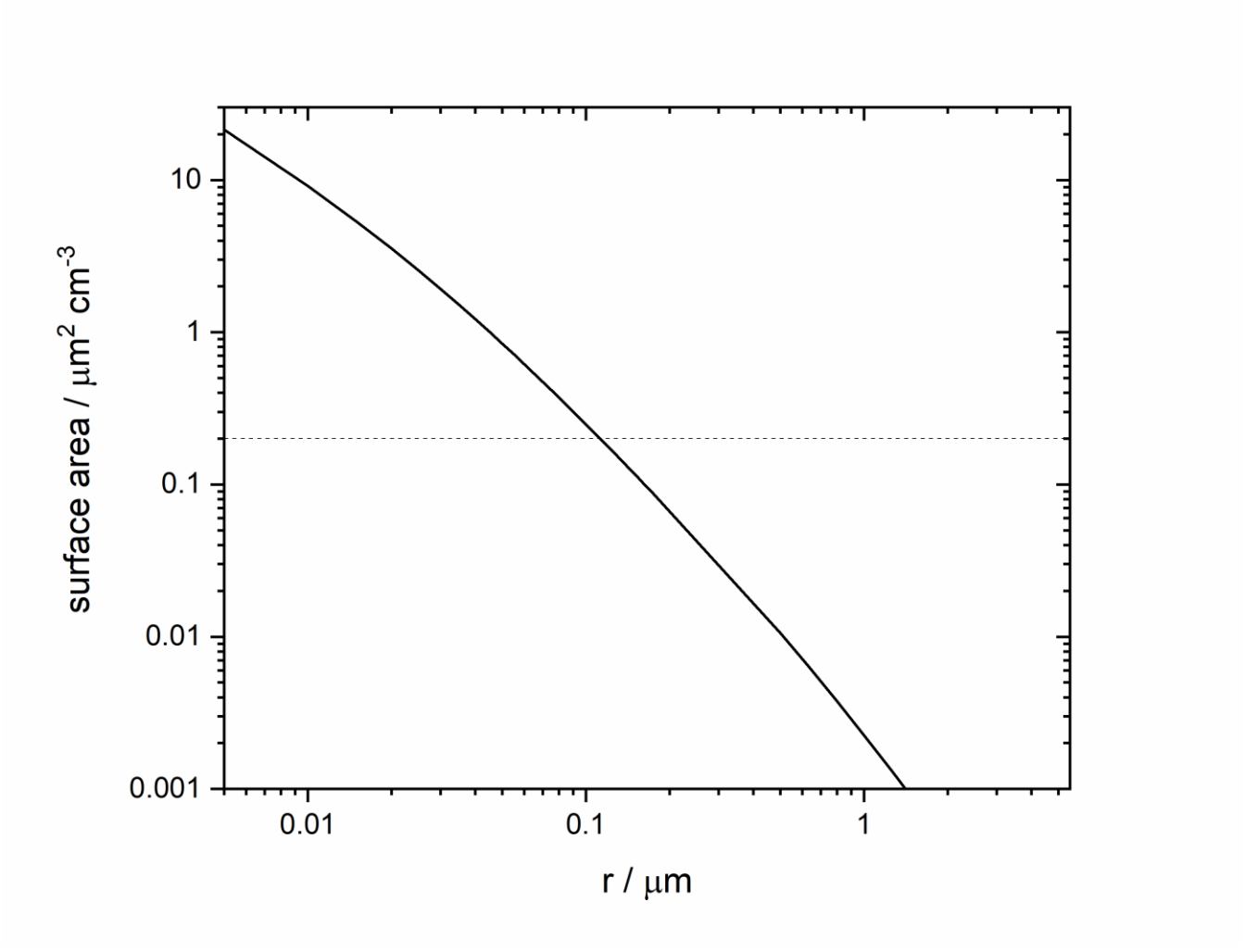

Figure 6: Surface area of meteoric fragments assuming that a reasonable upper limit of 137 ton day^{-1} fragment to the radius shown and sediment gravitationally to 20 km. Dashed horizontal line shows the 0.2 μm^2 cm^{-3} required to produce the lower limit of observed crystal numbers in water ice free PSCs.

Recent laboratory studies have suggested that meteorites heated to simulate the fragmentation process often become stronger (require more pressure for an atomic force microscope tip to break the surface) if somewhat more brittle (tip penetrates deeper once the surface is broken) (Bones et al., 2022). Recent stress testing of material from comet 67P suggests that the particles are made up of agglomerated fractals with highly non-spherical primary particle size of at least several hundred nm equivalent radius (Mannel et al., 2019). These studies do suggest a sub-set of loosely agglomerated, relatively weak cosmic dust which may fragment, though constraining the influx of such a material precisely enough for a quantitative comparison between nucleation by MSP and fragments is not currently possible.

https://doi.org/10.5194/acp-2022-598
Preprint. Discussion started: 29 August 2022


Atmospheric Chemistry and Physics Discussions

Based on these various analyses, some statements can be made about the potential for fragments to act as competitive heterogeneous nucleating particles in PSC. Firstly, micron-sized fragments, whilst they do reside in the lower stratosphere for time periods similar to the cloud lifetime, would require a very large meteoric flux to compete as nucleating particles. The upper end of estimates based on aircraft observations of large particles might allow for such high fluxes (Weigel et al., 2014), but they would be extremely difficult to reconcile with observations and modelling of dust in our solar system. Secondly, if observations from comet 67P can be generalised to all cosmic dust (Mannel et al., 2019), and the minimum fragment size is some hundreds of nm equivalent radius, a reasonable upper limit to the MIF is unlikely to be sufficient to contribute to crystallisation. Fragmentation to 100 nm radius would be required for our upper limit mass flux to produce our lower limit fragment surface area, and this is somewhat smaller than the primary particle size observed from comet 67P. Finally, fragmentation to 10s nm radius would be required to agree with MIF estimates of unablated material consistent with the zodiacal light, cosmic spherule collections and mesospheric metal fluxes to cause competitive nucleation (Carrillo-Sánchez et al., 2020). At these sizes particles would be carried by atmospheric circulation, concentrated in the mesosphere towards the winter pole and partially dissolve in acid droplets, much like MSPs. However, mechanical break up of particles to such small sizes is not commonly possible even under controlled laboratory conditions (Wang and Forssberg, 2006).

The micron-size particles observed by aircraft in the stratosphere, some of which have compositions suggesting an extra-terrestrial origin (Ebert et al., 2016), could be fragmented meteoroids. If the 0.1 ppbm of refractory (stable under an electron beam) particles observed in that study were all meteoric fragments of 0.5 µm radius they would have surface area of 0.03 $\mu m^2\ cm^{-3}$ and require a mass flux of 270 tons day^{-1}, however not all of these particles are meteoric. Balloon-borne collections of refractory particles have shown a factor of 5 less refractory particles (Deshler et al., 2003). Atmospheric modelling of the distribution of fragmented material of reasonable size would assist with determining whether these particles could be fragmented meteoroids, but more information about the incoming material and fragmentation process would still be required to reach a firm conclusion. Taking all of this into account, we conclude that it is unlikely that meteoric fragments contribute as NAT nucleating particles in PSCs.

4 Size dependent nucleation by meteoric smoke particles

We now explore whether MSPs in reasonable atmospheric concentrations and size distributions would have sufficient activity to explain observed cloud crystal number densities. Silica has been shown to nucleate NAT in the past (James et al., 2018; Bogdan et al., 2003). James et al. (2018) showed that fumed silica particles of around 6 nm nucleated NAT much less effectively than micron scaled particles of silica. It is well-known that the nucleating ability of a particular material decreases dramatically when the grain size approaches the size of the critical cluster, typically < 10 nm (Pruppacher and Klett, 1978). Given silica particles in the stratosphere have a size distribution with a mean size in the 10s of nanometers (Bigg, 2012), it seems reasonable that some of these particles might nucleate NAT in the stratosphere. In order to explore this possibility, we

https://doi.org/10.5194/acp-2022-598
Preprint. Discussion started: 29 August 2022


Atmospheric Chemistry and Physics Discussions

construct a nucleating particle (NP) size-dependent model using CNT (Pruppacher and Klett, 1978), and use our data on heterogeneous nucleation by MSP analogues with available thermodynamic data to constrain this model. We then combine this with atmospheric measurements of the size distribution of available material and back-trajectory temperature and NO_y profiles as in our previous work (James et al., 2018), thereby predicting the cloud crystal number density which can be compared with observations.

Equations E1-4 provide a kinetic framework to determine nucleation rates from thermodynamic quantities and the empirically determined contact angle, which relates to the activity of the nucleating particle surface. In the case of the nitric acid / water system, these thermodynamic quantities are not well established, but experimental observations do exist which allow their values to be constrained. The most important of these are the surface tension, σ, and the diffusion barrier, ΔF. Note here that because we observe significant nucleation above the NAD melting point, we assume that a NAT phase is nucleating, and that it has the thermodynamic properties observed for NAT nucleation reported in the literature (i.e. it is the same polymorph as was observed in those other experimental studies). We go on to show that this assumption provides an internally consistent explanation of a range of experimental data, indicating that it is reasonable.

4.1 Diffusion activation energies

The diffusion activation energy has been measured in stoichiometric (*i.e.* 3:1 H_2O:HNO_2) solution (Tisdale et al., 1997), and found to vary over 48.5-36.8 kJ mol^{-1} at 185-200 K. However, here we were able to determine a value at a more atmospherically relevant liquid concentration by using the temperature-dependent crystal grown rate in our experiments. The growth rate of the advancing crystal / liquid interface between video frames in cm s^{-1} was measured for crystals forming in droplets of 40 wt% HNO_3. An Arrhenius fit to these crystal growth rates is shown in Figure 7, resulting in a value measured between 182 and 207 K of 35.3 ± 4.3 kJ mol^{-1}, in agreement within error with the previous measurement. We note that both our and the literature value are somewhat higher than the 25 kJ mol^{-1} derived from measurements of HNO_3 diffusion coefficients on ice (Luo et al., 2003).

https://doi.org/10.5194/acp-2022-598
Preprint. Discussion started: 29 August 2022

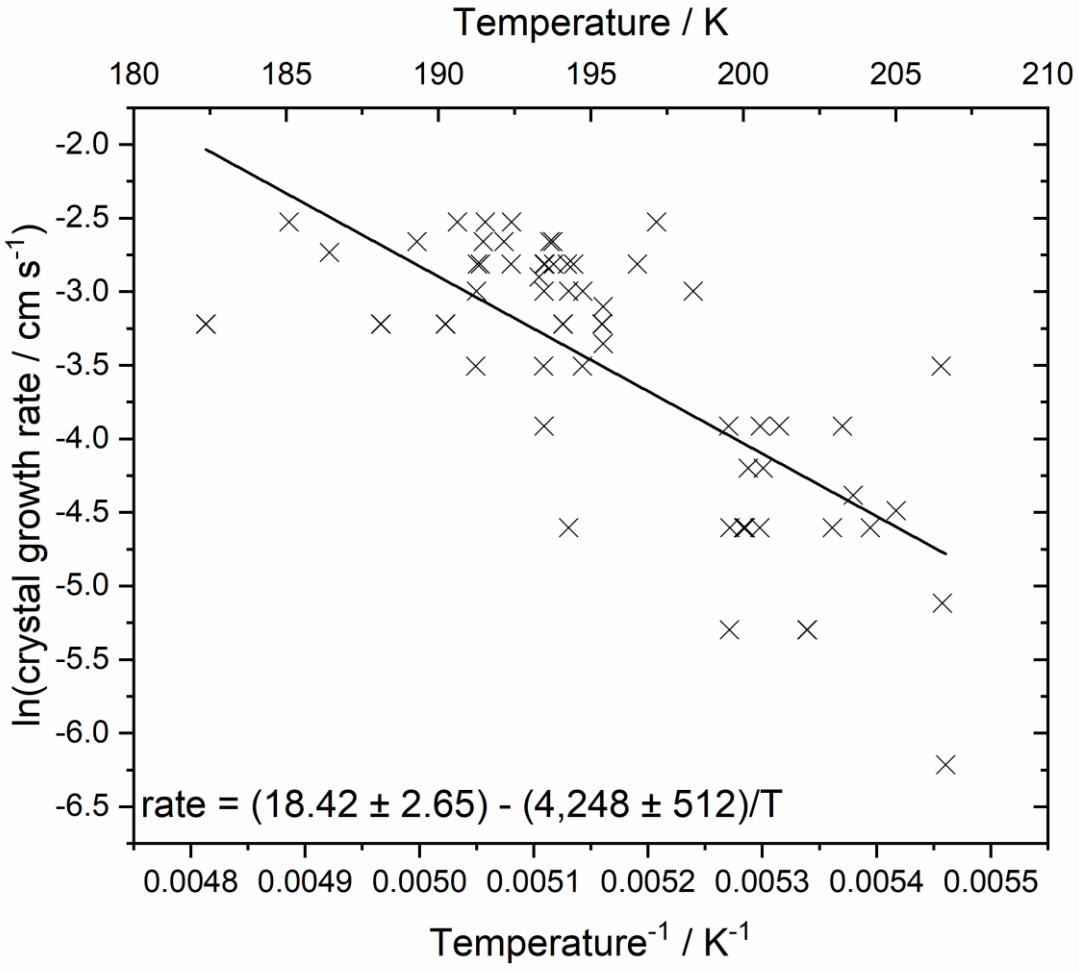

Figure 7: Arrhenius fit to crystal growth rate to determine diffusion barrier from 40 % HNO_3 liquid to crystalline NAT.

A number of factors may contribute to a relatively large scatter in this data. The orientation of the camera means that any growth out of the perpendicular (to the camera) plane of the slide will be neglected, leading to an underestimate of the true growth rate. Also, the latent heat generated will affect the droplet temperature such that there is a feedback between the droplet temperature and growth rate. However, the crystals appear to grow circularly (spherically) as opposed to e.g. cubic crystalline shapes. This implies that the diffusion of liquid material adding to the crystal is rate limiting rather than their ability to shed latent heat of crystallisation so from this perspective at least the growth rates provide a good measure of solution diffusion energies.

https://doi.org/10.5194/acp-2022-598
Preprint. Discussion started: 29 August 2022

Atmospheric Chemistry and Physics Discussions

335 **4.2 Surface energy of a NAT cluster**

The preferred method of deriving the interfacial energy between the nascent crystalline cluster and the liquid is through measurements of the temperature-dependent homogeneous nucleation of that crystalline phase (Koop and Murray, 2016). For nitric acid hydrates, there are relatively few measurements of homogeneous nucleation, and a number of different treatments of that data have been used. It has been noted that extrapolation of data from homogeneous experiments to atmospheric
340 conditions could be problematic since the dependence of the surface energy on saturation is unknown (Knopf et al., 2002). Here, rather than choosing an absolute value, we examine the values that can be derived from the literature and explore the sensitivity of our nucleation model within a range constrained by those values.

Before homogeneous nucleation measurements were available, the Turnbull correlation of the enthalpy of fusion to the surface tension was used to derive a value for NAT (MacKenzie et al., 1998). The authors in that study derived a value of 7 kJ mol^{-1}
345 (see their Figure 2) at 200 K. To convert this to a value per surface area, we take a surface molecular density from the 110 plane of β-NAT (Wood, 1999), which has four NAT molecules in a planar unit cell 9.4845 × 14.6836 Å (Taesler et al., 1975), giving a value of 0.03 ± 0.01 J m^{-2}. This is a rather indirect method; and relies on speculative assumptions, such as which crystal face is growing. However, it has the advantage that since the temperature-dependent enthalpies are known, a σ value can be determined at atmospherically-relevant temperatures.

350 Homogeneous nucleation of NAT has been observed experimentally in two studies (Bertram and Sloan, 1998;Salcedo et al., 2001). In both cases the authors report measured nucleation rates but do not derive σ values. These experimental data were used in a subsequent study to derive a σ_{NAT} value considering the incongruent (multiple component) nature of the NAT crystal and liquid (Djikaev and Ruckenstein, 2017). Here we re-analyse the experimental rate measurements using a linearised form of E1. We select the Tisdale et al. (1997) value for the diffusion activation energy, since it is more relevant to the concentrations
355 used in the homogeneous nucleation experiments, the temperature and saturation data from the homogeneous nucleation experiments, and a molar volume of 5.35 × 10^{-29} cm^3 mol^{-1}, based on a NAT density of 1.652 g cm^{-3}. The re-analysed results are shown in Figure 8, and all σ_{NAT} values are summarised in Table 2.

https://doi.org/10.5194/acp-2022-598
Preprint. Discussion started: 29 August 2022

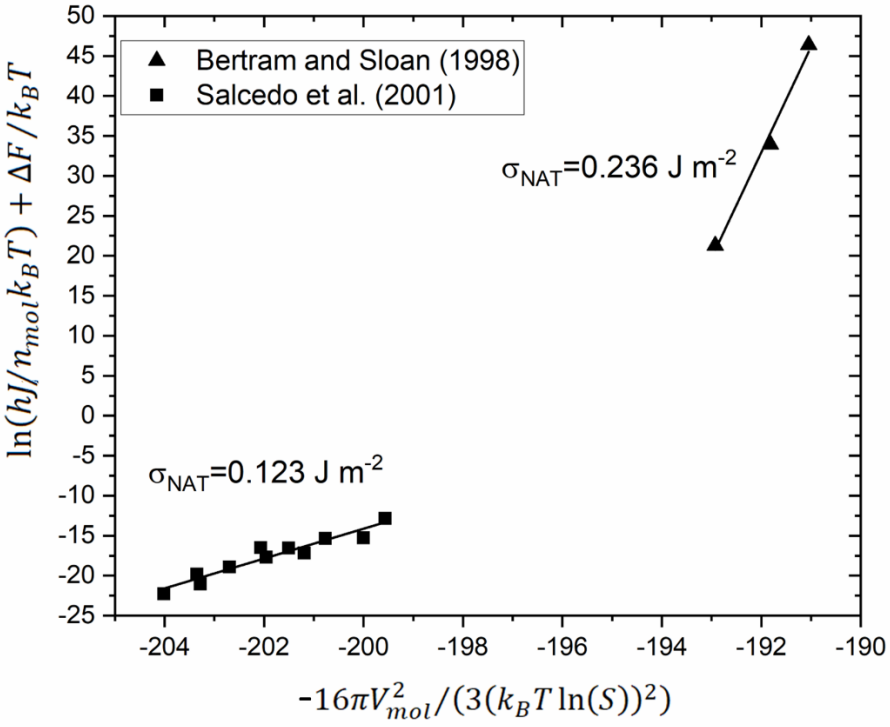

Figure 8: Reanalysis of measured homogeneous nucleation rates from Salcedo et al. (2001) (see their Figure 7) and Bertram and Sloan (1998). Axes represent the linearised form of E4 substituted into the equivalent of E1 for homogeneous nucleation (Murray et al., 2012). Linear regression fits and derived surface energies are shown.

These four estimates of the surface energy vary by a factor of eight. They are larger by a factor of 1.5-10 than current estimates of the value for water ice-liquid interface (Koop and Murray, 2016;Tarn et al., 2021). This seems reasonable since the interfacial energy is related to how alike the liquid and solid phases are, and NAT requires more molecules to rearrange than water ice and a greater disruption to the hydrogen bonding network at the interface. Because they were measured or derived for different conditions, and it is not known how the surface energy varies with temperature or saturation, we investigate the atmospheric implications of a range of possible interfacial energies based on these values and comparison to our experimental data on heterogeneous nucleation.

4.3 Contact angles

Given these physical parameters constrained by homogeneous nucleation rates, the heterogeneous activity of a substrate can then be quantified by constraining the contact angle, θ, using E1-4 and measured heterogeneous nucleation rates. For MSP, our previous heterogeneous nucleation experiments using fumed silica and fused quartz are well suited to this task (James et

https://doi.org/10.5194/acp-2022-598
Preprint. Discussion started: 29 August 2022


Atmospheric Chemistry and Physics Discussions

al., 2018). We found that fused quartz (crystalline quartz which has been melted and shock frozen to give an amorphous material) with a BET surface area of 4.85 m^2 g^{-1} and spherical equivalent particle radius of 240 nm nucleated crystallisation around 20 K warmer than a similar amount of fumed silica (a similarly amorphous material made by pyrolysis of silicon tetrachloride), which has a BET surface area of 195 m^2 g^{-1} and spherical equivalent particle radius of 5.8 nm.

Figure 9 shows fits of E1-4 for these two materials, using the diffusion barrier estimated from our observed temperature dependence of crystal growth rate (see Figure 7). Varying the diffusion barrier within uncertainty moves the predicted fraction frozen by several K for fused quartz, whilst the fumed silica fit is more sensitive. A range of σ_{NAT} values constrained by the homogeneous measurements were considered. For each σ_{NAT} value the experimental conditions of the fused quartz data were first used to find a θ which gave good agreement with the observed nucleation temperatures. The radius of the nucleating particle, r_{NP}, was taken as the spherical equivalent of the measured BET surface area; however, for fused quartz the calculated nucleation rate is insensitive to this quantity as the nucleating particle is significantly larger than the critical cluster size. This gave a paired θ for each σ_{NAT}, as shown in Table 2, and for σ_{NAT}=0.1 J m^{-2} as an example in Figure 9, the calculated nucleation rate is rather sensitive to θ, so the heterogeneous activity of the amorphous silica material could be quantified within a small range. Making the assumption that the fumed silica has similar nucleation properties, and that its different nucleation temperatures are due only to its smaller particle size, we then use these paired θ and σ_{NAT} values with a varied r_{NP} to reproduce the observed nucleation rates of fumed silica suspensions. The resulting particle sizes, shown in Table 2, give a further check on the physical reasonability of the thermodynamic data. Some variability from the size estimated from BET is reasonable: firstly because BET assumes that particles are uniformly spherical; and secondly because the silica can partially dissolve and reprecipitate in acid solution to give a change in particle size. In addition, we assigned a single contact angle to describe nucleation on these silica surfaces. The fact that the CNT curves in Fig 9 reproduce the steepness of the experimental curves implies that this is a reasonable assumption, despite the fact that in many heterogeneous nucleating systems a distribution of contact angles is required to describe the data (Herbert et al., 2015).

Figure 9 shows self-consistency between measurements of nucleation activity on these two chemically similar materials. This suggests that size-dependent CNT is a good model for this process, and that the laboratory measurements of heterogeneous nucleating activity are a good way to constrain the physical system and thereby quantify the atmospheric process.

https://doi.org/10.5194/acp-2022-598
Preprint. Discussion started: 29 August 2022

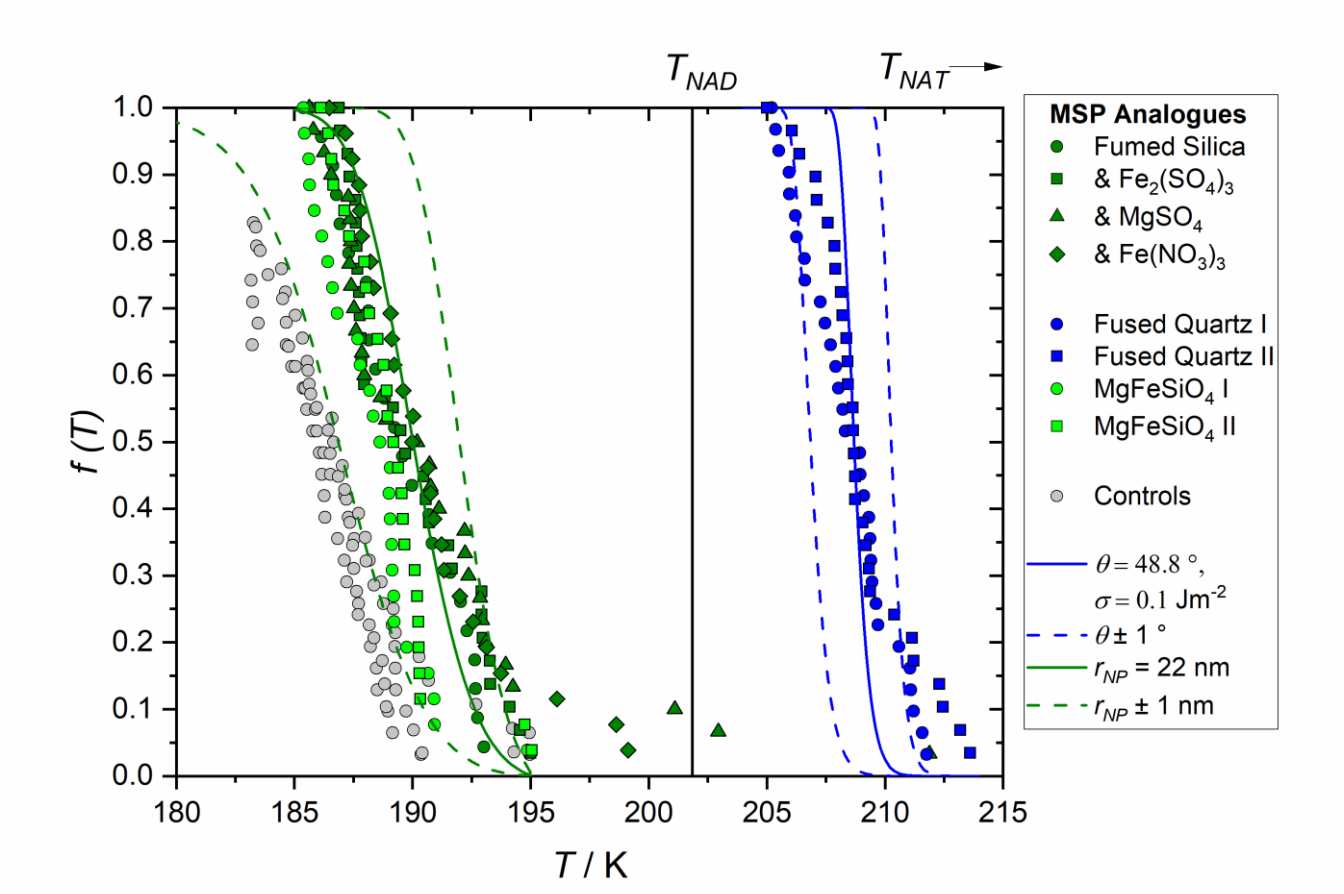

Figure 9: Meteoric smoke analogue fraction frozen as measured in our previous work (points, (James et al., 2018)) and as modelled here using the size dependent nucleation rate parameterisation described by equations E1 to E4, lines. Grey points show the instrument background. Blue data shows nucleation measured on fused quartz (BET surface area 4.85 m^2 g^{-1}) and green data fumed silica (BET surface area 195 m^2 g^{-1}). Fused quartz data is used to constrain the contact angle for a given surface energy since this is insensitive to particle size, blue solid line shows 0.1 J m^{-2} as an example, and blue dashed lines show the sensitivity to the contact angle. These paired θ and σ values are then used to determine the nucleating particle radius, r_{NP}, which gives a good fit (solid green line) to the fumed silica data, again shown here for σ_{NAT}=0.1 J m^{-2}, dashed green lines show the sensitivity to the particle size.

We now explore the sensitivity of the parameterisation to the input parameters. The interfacial energy value determined by the Turnbull correlation resulted in a nucleation rate too fast at temperatures warmer than 215 K to explain the observed fused quartz nucleation data, even assuming homogeneous nucleation. We therefore recommend a lower limit value for σ_{NAT} of 0.05 J m^{-2}, which produces a good fit to both amorphous silica datasets with θ = 100 ° and r_{NP} = 4 nm, 30% smaller than the BET spherical equivalent size of the fumed silica. Both our and Djikaev and Ruckenstein (2017)'s analysis of homogeneous nucleation measured by Salcedo et al. (2001) place σ_{NAT} between 0.1 J m^{-2} and 0.15 J m^{-2}. The value we derive from the measurements of Bertram and Sloan (1998) is 0.236 mJ m^{-2}, somewhat higher than the other constraints. We do not test a

https://doi.org/10.5194/acp-2022-598
Preprint. Discussion started: 29 August 2022

Atmospheric Chemistry and Physics Discussions

range of values which includes our analysis of the Bertram and Sloan (1998) data since there are fewer data points on which to base this value and controlling the conditions in flow tube experiments such as those of Bertram and Sloan (1998) is known to be challenging. Such a large σ_{NAT} would require a very active (small contact angle) amorphous silica material to explain our observed nucleation rates. For example, using a slightly different application of CNT, Hoyle et al. (2013) found that a minimum contact angle of 43° gave a good agreement with observed cloud. Note that we do not rule out the possibility that σ_{NAT} might be this high, but we consider it unlikely. We therefore go on to examine the atmospheric implications of this model of the heterogeneous NAT nucleating activity of amorphous silica from MSPs, investigating a range of interfacial energy values from 0.05 to 0.15 Jm^{-2}, and finally compare the likely atmospheric impacts of MSPs and fragments.

Table 2: Surface energy, σ_{NAT}, values in the literature or derived from literature nucleation rate data

σ_{NAT} / J m^{-2}	Valid T / K	Valid $[HNO_3]$ / $wt\%$	θ from fused quartz experiments/ °	r_{NP} from fumed silica / nm	reference
0.03	200	54	unphysical	N/A	MacKenzie et al. (1998)
0.11	155-180	50-64	45	23	Djikaev and Ruckenstein (2017)
0.123	175-180	50-64	41	24	Derived here from Salcedo et al. (2001)
0.236	155-175	54	24.4	27	Derived here from Bertram and Sloan (1998)
Reasonable range of values chosen here for atmospheric comparison:					
0.05	210-185	40	100	4	
0.1	210-185	40	48.8	22	
0.15	210-185	40	34.9	25	

4.4 The likely nature of MSP in ternary acid solutions

It is well established that acid processing of MSPs results in dissolution of most metal components, leaving silica and alumina solids in suspension (Murphy et al., 2014;Saunders et al., 2012). Indeed the similar activity of synthetic MSP analogues to fumed silica measured in James et al. (2018) suggests that acid processing leaves these materials alike.

https://doi.org/10.5194/acp-2022-598
Preprint. Discussion started: 29 August 2022


Atmospheric Chemistry and Physics Discussions

In the presence of H_2SO_4, these suspensions were found to form a gel within several hours at room temperature, which showed no nucleation activity above the instrument baseline (data not shown). Silica suspensions here contained approximately 2.5 wt% silica, around a factor of five larger than atmospheric concentrations (Cziczo et al., 2001). Silica gelation is also known to be strongly temperature dependent (Colby et al., 1986). This suggests that this is an artifact of the laboratory method, and that stratospheric droplets would not form a gel. Indeed, if the silica particles formed a gel throughout the droplet, the silica would be evenly distributed and atmospheric single particle mass spectrometers would detect a narrow distribution of ion ratios for silicon, as they do for e.g. iron and nickel (Murphy et al., 2014). Electron microscopy of collected particles has shown the presence of agglomerated spherical particles, which is also not consistent with gel formation (Ebert et al., 2016;Bigg, 2012).

4.5 Atmospherically available MSP

To implement this size dependent parameterisation of heterogeneous NAT nucleation by amorphous silica from MSPs, we combine modelling of atmospheric MSP chemistry and transport with observed aerosol size distributions. The most recent estimate of the ablated meteoroid mass, which provides the material from which MSPs form, is 8.3 tons day^{-1} (Carrillo-Sánchez et al., 2020). Modelling of the growth, atmospheric circulation and entrainment of these particles in stratospheric sulfate aerosol suggests an average mass concentration of $(1.5 \pm 0.5) \times 10^{-15}$ g cm^{-3} at 67 °N latitude, 70 hPa altitude in February (James et al., 2018). We then consider a size distribution as measured for particles collected in the lower and middle stratosphere, which were found to have little variation with altitude (Bigg, 2012). By using the observed size distribution to define the smoke particle size distribution and normalising to the mass concentration from WACCM modelling, we obtain the "initial" size distribution shown in Figure 10. This distribution contains an integrated number concentration of 23.5 particles cm^{-3}, similar to commonly applied estimates of around 20 cm^{-3} for the number of liquid aerosol in the stratosphere (Hoyle et al., 2013). The integrated particle surface area is 0.08 μm^2 cm^{-3}, approximately a factor of two less than applied by assuming mono-disperse particles in James et al. (2018).

https://doi.org/10.5194/acp-2022-598
Preprint. Discussion started: 29 August 2022

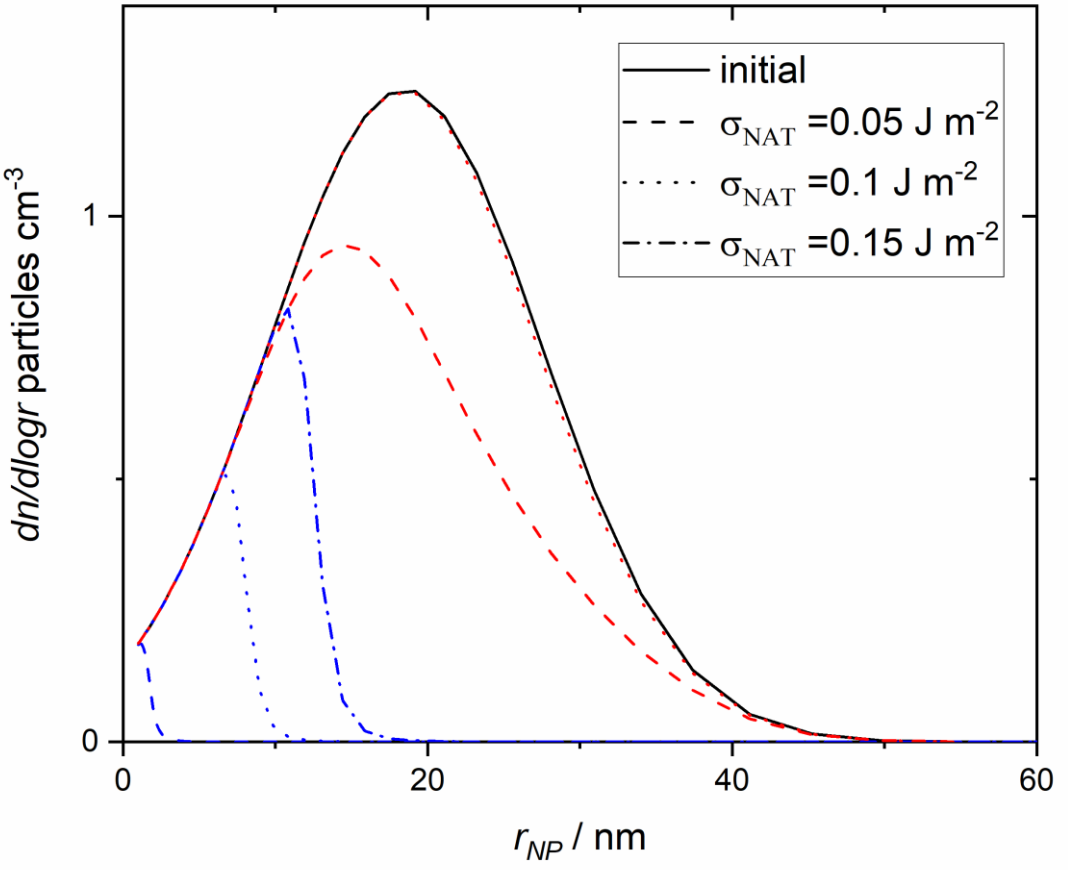

Figure 10: Size distribution of MSPs. Initial (black, solid line) distribution and that of the particles that "survive" (do not cause nucleation) is shown. Line style differentiates assumed surface energy values, blue data shows values assuming 15 ppmv HNO_3 and red values 10 ppmv. The surviving distribution assuming 10 ppbv HNO_3 and σ_{NAT} = 0.15 is indistinguishable from the initial distribution on this scale.

4.6 Simulated atmospheric nucleation by MSPs

We now combine this size-dependent nucleation parameterisation with the distribution of available MSPs and the same atmospheric trajectory model we applied previously (James et al., 2018). The nucleation rates and resulting crystal number concentrations are calculated by assuming that each MSP occupies a separate liquid droplet, *i.e.* that each can cause a single nucleation event. We do not account for processes such as the transfer of material from surviving droplets to the nucleated crystals, or the sedimentation of the growing crystals from the modelled volume. As long as the equilibrium vapour pressure over the NAT crystal is lower than over the droplet (*i.e.* the atmosphere is saturated with respect to NAT), there will be a net

https://doi.org/10.5194/acp-2022-598
Preprint. Discussion started: 29 August 2022


Atmospheric Chemistry and Physics Discussions

transfer of HNO_3 from the remaining liquid to the growing crystal. This results in reduced HNO_3 concentration and saturation in the liquid, reducing subsequent nucleation. The resulting crystals can grow to micron or even 10s micron scales, causing them to sediment out of the NAT saturated airmass (Fueglistaler et al., 2002). These cloud micro-physical processes require a detailed microphysical model to address, hence are out of scope here. Carslaw et al. (2002), found that a time step of 30 minutes or less was required to accurately account for these processes in clouds with particle concentrations of 10^{-4} cm^{-3} or less, so their effects could be significant across the 18 hours of our trajectory model. By neglecting this we can only produce an upper limit to the number of crystals which could form in the atmosphere. As a result of this limitation, we aim here only to decide whether MSPs could be active enough to explain the observations, not to exactly reproduce them.

The results are compared to observed crystal concentrations in the atmosphere (Voigt et al., 2005), and other parameterisations of nucleation, in Figure 11. Assuming 15 ppmv HNO_3, more than half of the MSP particles are able to nucleate NAT within the trajectory timescale. The surviving distribution of MSPs (which do not cause nucleation within this trajectory model) is shown by dashed lines in Figure 10, and demonstrates that when the size of the nucleating particle is taken into account, there is essentially a threshold below which particles are too small to cause nucleation. The threshold size depends on the value taken for the interfacial energy. For 10 ppbv HNO_3, less nucleation is observed, though crystal number concentrations still significantly exceed those measured in the atmosphere. The final number concentration of crystals is a strong function of the chosen value of σ_{NAT}.

https://doi.org/10.5194/acp-2022-598
Preprint. Discussion started: 29 August 2022

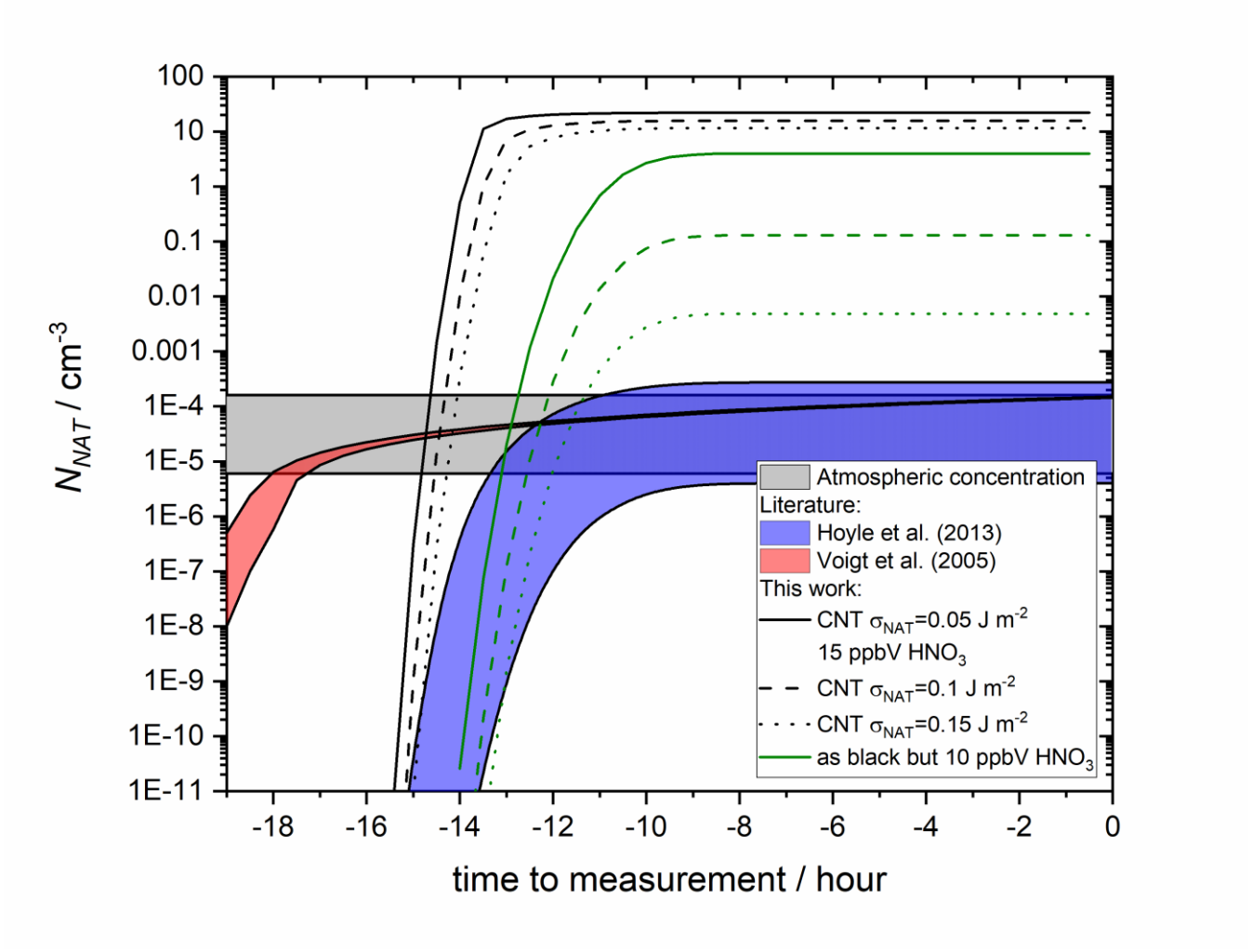

Figure 11: NAT particle production using a temperature profile based on stratospheric observations. See James et al. (2018) Figure 6(a) for corresponding temperature and saturations. S_{NAX} were calculated at 70 hPa assuming 5 ppmV H_2O, 0.1 ppbV H_2SO_4 and 10 (minimum of ranges and blue lines) to 15 (maximum of ranges and black lines) ppbV HNO_3. Growth, sedimentation of particles and removal of HNO_3 are not taken into account. These processes will limit the number of NAT particles that can nucleate by reducing the HNO_3 concentration and NAT saturation in remaining droplets, hence our predicted NAT number concentrations are an upper limit. Predicted N_{NAT} based on nucleation parameterisations from this work compared to James et al. (2018) and estimated surface areas and size distributions of meteoric smoke particles (MSPs) as well as two literature parameterisations (Voigt et al., 2005;Hoyle et al., 2013). The CNT parameterisation produced in this work is shown for a range of surface energy (σ_{NAT}) values differentiated by line type, using paired contact angles constrained by heterogenous nucleation experiments.

The nature of MSPs in atmospheric liquid droplets may also contribute to this overestimation. Here we assume that the particles in our size distribution are dispersed evenly and each particle is able to nucleate a crystal. In fact this distribution relates to the size of primary grains that were observed as agglomerates in atmospheric droplets (Bigg, 2012). This means that more than one nucleating particle would be removed with each nucleation event, and the final number of crystals would be lower. Voigt

https://doi.org/10.5194/acp-2022-598
Preprint. Discussion started: 29 August 2022


Atmospheric Chemistry and Physics Discussions

et al. (2005) measured a concentration of 10 particles cm^{-3} (liquid droplets) on the flights to which these back trajectories relate. A number of studies have shown that typically 50-80 % of stratospheric liquid aerosol contains a refractory core (Weigel et al., 2014;Schneider et al., 2021;Murphy et al., 2021). This would suggest that at least 5 particles cm^{-3} contained an MSP, with an average of 4.7 primary particles per droplet, randomly sampled from the total distribution. This would mean that any nucleation event would remove all primary particles in that liquid droplet, with a linear reduction in the final number concentration of crystals. For the trajectory calculated using 10 ppbV HNO_3 and σ_{NAT} = 0.15, this would result in 10^{-3} crystals cm^{-3}, still significantly higher than the measured concentration.

We conclude that nano-scale amorphous silica particles formed by dissolution of MSPs in stratospheric sulfuric acid droplets are sufficiently active heterogeneous nucleators of NAT to explain observed cloud crystallisation warmer than the H_2O ice melting point. This could have significant implications for particularly early season Antarctic or Arctic clouds where temperatures may not be cold enough for water ice to form, and hence impact on the buildup of ozone-destroying species throughout the winter and eventually on ozone depletion.

We recommend that the CNT parameterisation presented here is deployed in atmospheric models of PSC crystallisation and ozone depletion and the effect of varying the NAT/liquid interfacial energy investigated. In a model that described droplet-to-crystal material transfer, particle growth and sedimentation, the number of crystals formed would reduce towards the observed values. Additionally, if our observation that the number of crystals formed is influenced by the input value of σ_{NAT} holds, the "atmospheric laboratory" may now be an effective domain to further constrain this important thermodynamic quantity. The system is complex, with remaining uncertainties in a number of thermodynamic quantities, so that it is difficult to predict which effect will control the number of crystals formed under any given atmospheric conditions.

5. Conclusions

In the laboratory, analogues for meteoric fragments can nucleate nitric acid hydrate crystals in ternary solution droplets with compositions relevant to Polar Stratospheric Clouds. This nucleation shows complex behaviour, but in some cases is resistant to deactivation by both nitric and sulfuric acids in atmospheric concentrations. This was shown previously (James et al., 2018), but we have now extended these studies to include sulfuric acid and annealing of meteoric fragments at temperatures experienced during entry into the atmosphere. However, consideration of the latest understanding of meteoric fragmentation and sedimentation processes suggest that there is unlikely to be sufficient input flux of fragmenting meteoroids in order for this material to heterogeneously nucleate observed crystal numbers in PSC. Hence, while any fragmented of meteoroids could nucleate NAT in the polar stratosphere there are unlikely to be sufficient numbers to nucleate the majority of observed NAT crystals under any conditions and we conclude some other nucleation pathway must dominate.

https://doi.org/10.5194/acp-2022-598
Preprint. Discussion started: 29 August 2022


Atmospheric Chemistry and Physics Discussions

We propose that acid processed meteoric smoke (i.e. silica) can nucleate NAT, despite its small size. We constrain a model of nucleating particle size-dependent classical nucleation theory by combining existing laboratory data on diffusion barriers under homogeneous conditions, surface free energy, heterogeneous nucleation activity of amorphous silica materials, and a new measurement of diffusion barriers under heterogeneous nucleation conditions. Application of this parameterisation to atmospheric cloud observations overpredicts the resulting crystal number densities. The comparison carried out here uses state-of-the art knowledge of MSPs in the atmosphere, which appears robust, but neglects the growth and sedimentation of particles after nucleation, which would reduce the total crystal number. This suggests that MSPs are sufficiently active to explain observed crystal numbers in polar stratospheric clouds, and that application of our constrained nucleation activity in more complete atmospheric models could now provide an improved understanding of PSC microphysics and ultimately ozone depletion.

This work shows that the modelling of crystal nucleation in early season PSCs and the resulting ozone depletion relies on the nucleation of nitric acid hydrate crystals on meteoric smoke. Hence, in order to quantitatively predict the effect of a changing climate, long-term ozone recovery or events such as volcanic eruptions on stratospheric ozone an adequate understanding of the meteoric input, the sources of meteoric material in the solar system and how these interact with Earth's atmosphere, the production of meteoric smoke in the mesosphere and its transport through the mesosphere and stratosphere are all needed.

Acknowledgements

This work forms part of the MeteorStrat project funded by the UK Natural Environment Research Council (grant number NE/R011222/1).

References

Adachi, K., Oshima, N., Takegawa, N., Moteki, N., and Koike, M.: Meteoritic materials within sulfate aerosol particles in the troposphere are detected with transmission electron microscopy, Comm.s Earth & Env., 3, 134, 10.1038/s43247-022-00469-8, 2022.

Bertram, A. K., and Sloan, J. J.: The nucleation rate constants and freezing mechanism of nitric acid trihydrate aerosol under stratospheric conditions, J. Geophys. Res.: Atmos., 103, 13261-13265, https://doi.org/10.1029/98JD00921, 1998.

Bigg, K. E.: Sources of insoluble inclusions in stratospheric sulfate particles, Meteorit. & Plan. Sci., 47, 799-805, https://doi.org/10.1111/j.1945-5100.2012.01346.x, 2012.

Bogdan, A., Molina, M. J., Kulmala, M., MacKenzie, A. R., and Laaksonen, A.: Study of finely divided aqueous systems as an aid to understanding the formation mechanism of polar stratospheric clouds: Case of HNO_3/H_2O and H_2SO_4/H_2O systems, J. Geophys. Res.: Atmos., 108, 4302, 10.1029/2002JD002605, 2003.

Bones, D. L., Carrillo Sánchez, J.-D., Connell, S. D. A., Kulak, A. N., Mann, G. W., and Plane, J. M. C.: Ablation rates of organic compounds in cosmic dust and resulting changes in mechanical properties during atmospheric entry, Earth Space Sci., 9, e2021EA001884, https://doi.org/10.1029/2021EA001884, 2022.

https://doi.org/10.5194/acp-2022-598
Preprint. Discussion started: 29 August 2022

Atmospheric Chemistry and Physics Discussions

Brakebusch, M., Randall, C. E., Kinnison, D. E., Tilmes, S., Santee, M. L., and Manney, G. L.: Evaluation of Whole Atmosphere Community Climate Model simulations of ozone during Arctic winter 2004–2005, J. Geophy. Res.: Atmos., 118, 2673-2688, 10.1002/jgrd.50226, 2013.

Brooke, J. S. A., Feng, W., Carrillo-Sánchez, J. D., Mann, G. W., James, A. D., Bardeen, C. G., Marshall, L., Dhomse, S. S., and Plane, J. M. C.: Meteoric smoke deposition in the polar regions: A comparison of measurements with global atmospheric models, J. Geophys. Res.: Atmos., 122, 11,112-111,130, 10.1002/2017jd027143, 2017.

Carrillo-Sánchez, J. D., Gómez-Martín, J. C., Bones, D. L., Nesvorný, D., Pokorný, P., Benna, M., Flynn, G. J., and Plane, J. M. C.: Cosmic dust fluxes in the atmospheres of Earth, Mars, and Venus, Icarus, 335, 113395, https://doi.org/10.1016/j.icarus.2019.113395, 2020.

Carslaw, K. S., Peter, T., and Clegg, S. L.: Modeling the composition of liquid stratospheric aerosols, Rev. Geophys., 35, 125-154, https://doi.org/10.1029/97RG00078, 1997.

Carslaw, K. S., Peter, T., Bacmeister, J. T., and Eckermann, S. D.: Widespread solid particle formation by mountain waves in the Arctic stratosphere, J. Geophys. Res.: Atmos., 104, 1827-1836, https://doi.org/10.1029/1998JD100033, 1999.

Carslaw, K. S., Kettleborough, J. A., Northway, M. J., Davies, S., Gao, R.-S., Fahey, D. W., Baumgardner, D. G., Chipperfield, M. P., and Kleinböhl, A.: A vortex-scale simulation of the growth and sedimentation of large nitric acid hydrate particles, J. Geophys. Res.: Atmos., 107, SOL 43-41-SOL 43-16, https://doi.org/10.1029/2001JD000467, 2002.

Clarke, R., Jarosevich, E., Mason, B., Nelen, J., Gomez, M., and Hyde, J. R.: The Allende, Mexico, Meteoroite Shower, Smithsonian Institution Press, Washington, 1971.

Clegg, S. L., Brimblecombe, P., and Wexler, A. S.: Thermodynamic model of the system H^+–NH_4^+–SO_4^{2-}–NO_3^-–H_2O at tropospheric temperatures, J. Phys. Chem. A, 102, 2137-2154, 10.1021/jp973042r, 1998.

Colby, M. W., Osaka, A., and Mackenzie, J. D.: Effects of temperature on formation of silica gel, J. Non-Crystalline Solids, 82, 37-41, https://doi.org/10.1016/0022-3093(86)90108-0, 1986.

Cziczo, D. J., Thomson, D. S., and Murphy, D. M.: Ablation, flux, and atmospheric implications of meteors inferred from stratospheric aerosol, Science, 291, 1772-1775, 10.1126/science.1057737, 2001.

Deshler, T., Hervig, M. E., Hofmann, D. J., Rosen, J. M., and Liley, J. B.: Thirty years of in situ stratospheric aerosol size distribution measurements from Laramie, Wyoming (41°N), using balloon-borne instruments, J. Geophys. Res.: Atmos., 108, https://doi.org/10.1029/2002JD002514, 2003.

Dhomse, S. S., Saunders, R. W., Tian, W., Chipperfield, M. P., and Plane, J. M. C.: Plutonium-238 observations as a test of modeled transport and surface deposition of meteoric smoke particles, Geophys. Res. Lett., 40, 4454-4458, 2013.

Djikaev, Y. S., and Ruckenstein, E.: Free energy of formation of a crystal nucleus in incongruent solidification: Implication for modeling the crystallization of aqueous nitric acid droplets in polar stratospheric clouds, J. Chem. Phys., 146, 134709, 10.1063/1.4979069, 2017.

Ebert, M., Weigel, R., Kandler, K., Günther, G., Molleker, S., Grooß, J. U., Vogel, B., Weinbruch, S., and Borrmann, S.: Chemical analysis of refractory stratospheric aerosol particles collected within the arctic vortex and inside polar stratospheric clouds, Atmos. Chem. Phys., 16, 8405-8421, 10.5194/acp-16-8405-2016, 2016.

Engel, I., Luo, B. P., Pitts, M. C., Poole, L. R., Hoyle, C. R., Grooß, J. U., Dörnbrack, A., and Peter, T.: Heterogeneous formation of polar stratospheric clouds – Part 2: Nucleation of ice on synoptic scales, Atmos. Chem. Phys., 13, 10769-10785, 10.5194/acp-13-10769-2013, 2013.

Fahy, W. D., Maters, E. C., Giese Miranda, R., Adams, M. P., Jahn, L. G., Sullivan, R. C., and Murray, B. J.: Volcanic ash ice nucleation activity is variably reduced by aging in water and sulfuric acid: the effects of leaching, dissolution, and precipitation, Env. Sci.: Atmos., 10.1039/D1EA00071C, 2022.

https://doi.org/10.5194/acp-2022-598
Preprint. Discussion started: 29 August 2022

Atmospheric Chemistry and Physics Discussions

Frankland, V. L., James, A. D., Feng, W., and Plane, J. M. C.: The uptake of HNO_3 on meteoric smoke analogues, J. Atmos. Sol.-Terr. Phys., 127, 150-160, http://dx.doi.org/10.1016/j.jastp.2015.01.010, 2015.

Frey, M., Didzoleit, H., Gainaru, C., and Böhmer, R.: Dynamics in glass forming sulfuric and nitric acid hydrates, J. Phys. Chem. B, 117, 12164-12174, 10.1021/jp407588j, 2013.

Fueglistaler, S., Luo, B. P., Buss, S., Wernli, H., Voigt, C., Müller, M., Neuber, R., Hostetler, C. A., Poole, L. R., Flentje, H., Fahey, D. W., Northway, M. J., and Peter, T.: Large NAT particle formation by mother clouds: Analysis of SOLVE/THESEO-2000 observations, Geophys. Res. Letts., 29, 52-51-52-54, https://doi.org/10.1029/2001GL014548, 2002.

Grooß, J. U., Engel, I., Borrmann, S., Frey, W., Günther, G., Hoyle, C. R., Kivi, R., Luo, B. P., Molleker, S., Peter, T., Pitts, M. C., Schlager, H., Stiller, G., Vömel, H., Walker, K. A., and Müller, R.: Nitric acid trihydrate nucleation and denitrification in the Arctic stratosphere, Atmos. Chem. Phys., 14, 1055-1073, 10.5194/acp-14-1055-2014, 2014.

Grothe, H., Tizek, H., and Ortega, I. K.: Metastable nitric acid hydrates-possible constituents of polar stratospheric clouds?, Faraday Disc., 137, 223-234, 2008.

Holden, M. A., Whale, T. F., Tarn, M. D., O'Sullivan, D., Walshaw, R. D., Murray, B. J., Meldrum, F. C., and Christenson, H. K.: High-speed imaging of ice nucleation in water proves the existence of active sites, Science Advances, 5, eaav4316, doi:10.1126/sciadv.aav4316, 2019.

Hoyle, C. R., Engel, I., Luo, B. P., Pitts, M. C., Poole, L. R., Grooß, J. U., and Peter, T.: Heterogeneous formation of polar stratospheric clouds – Part 1: Nucleation of Nitric Acid Trihydrate (NAT), Atmos. Chem. Phys., 13, 9577-9595, 2013.

Jacobson, M.: Fundamentals of atmospheric modeling, 2nd edn Cambridge University Press, Cambridge University Press, New York, NY, 2005.

James, A. D., Moon, D. R., Feng, W. H., Lakey, P. S. J., Frankland, V. L., Heard, D. E., and Plane, J. M. C.: The uptake of HO_2 on meteoric smoke analogues, J. Geophys. Res.-Atmospheres, 122, 554-565, 10.1002/2016jd025882, 2017.

James, A. D., Brooke, J. S. A., Mangan, T. P., Whale, T. F., Plane, J. M. C., and Murray, B. J.: Nucleation of nitric acid hydrates in polar stratospheric clouds by meteoric material, Atmos. Chem. Phys., 18, 4519-4531, 10.5194/acp-18-4519-2018, 2018.

Knopf, D. A., Koop, T., Luo, B. P., Weers, U. G., and Peter, T.: Homogeneous nucleation of NAD and NAT in liquid stratospheric aerosols: insufficient to explain denitrification, Atmos. Chem. Phys., 2, 207-214, 10.5194/acp-2-207-2002, 2002.

Koop, T., and Murray, B. J.: A physically constrained classical description of the homogeneous nucleation of ice in water, J. Chem. Phys., 145, 211915, 10.1063/1.4962355, 2016.

Kremser, S., Thomason, L. W., von Hobe, M., Hermann, M., Deshler, T., Timmreck, C., Toohey, M., Stenke, A., Schwarz, J. P., Weigel, R., Fueglistaler, S., Prata, F. J., Vernier, J.-P., Schlager, H., Barnes, J. E., Antuña-Marrero, J.-C., Fairlie, D., Palm, M., Mahieu, E., Notholt, J., Rex, M., Bingen, C., Vanhellemont, F., Bourassa, A., Plane, J. n. M. C., Klocke, D., Carn, S. A., Clarisse, L., Trickl, T., Neely, R., James, A. D., Rieger, L., Wilson, J. C., and Meland, B.: Stratospheric aerosol—Observations, processes, and impact on climate, Reviews of Geophysics, 54, 278-335, 10.1002/2015rg000511, 2016.

Kumar, A., Marcolli, C., and Peter, T.: Ice nucleation activity of silicates and aluminosilicates in pure water and aqueous solutions – Part 3: Aluminosilicates, Atmos. Chem. Phys., 19, 6059-6084, 10.5194/acp-19-6059-2019, 2019.

Lawrence, Z. D., Perlwitz, J., Butler, A. H., Manney, G. L., Newman, P. A., Lee, S. H., and Nash, E. R.: The remarkably strong arctic stratospheric polar vortex of winter 2020: Links to record-breaking Arctic oscillation and ozone loss, J. Geophys. Res.: Atmos., 125, e2020JD033271, 10.1029/2020jd033271, 2020.

Love, S. G., and Brownlee, D. E.: A Direct Measurement of the Terrestrial Mass Accretion Rate of Cosmic Dust, Science, 262, 550-553, doi:10.1126/science.262.5133.550, 1993.

Luo, B. P., Voigt, C., Fueglistaler, S., and Peter, T.: Extreme NAT supersaturations in mountain wave ice PSCs: A clue to NAT formation, J. Geophy. Res.: Atmos., 108, 4441, https://doi.org/10.1029/2002JD003104, 2003.

MacKenzie, A. R., Laaksonen, A., Batris, E., and Kulmala, M.: The Turnbull correlation and the freezing of stratospheric aerosol droplets, J. Geophys. Res.: Atmos., 103, 10875-10884, https://doi.org/10.1029/98JD00169, 1998.

Mann, G. W., Carslaw, K. S., Chipperfield, M. P., Davies, S., and Eckermann, S. D.: Large nitric acid trihydrate particles and denitrification caused by mountain waves in the Arctic stratosphere, J. Geophys. Res.: Atmos., 110, 10.1029/2004JD005271, 2005.

Mannel, T., Bentley, M. S., Boakes, P. D., Jeszenszky, H., Ehrenfreund, P., Engrand, C., Koeberl, C., Levasseur-Regourd, A. C., Romstedt, J., Schmied, R., Torkar, K., and Weber, I.: Dust of comet 67P/Churyumov-Gerasimenko collected by Rosetta/MIDAS: classification and extension to the nanometer scale, A&A, 630, A26, 2019.

Murphy, D. M., Froyd, K. D., Schwarz, J. P., and Wilson, J. C.: Observations of the chemical composition of stratospheric aerosol particles, Quart. J. Royal Met. Soc., 140, 1269-1278, 2014.

Murphy, D. M., Froyd, K. D., Bourgeois, I., Brock, C. A., Kupc, A., Peischl, J., Schill, G. P., Thompson, C. R., Williamson, C. J., and Yu, P.: Radiative and chemical implications of the size and composition of aerosol particles in the existing or modified global stratosphere, Atmos. Chem. Phys., 21, 8915-8932, 10.5194/acp-21-8915-2021, 2021.

Murray, B. J., O'Sullivan, D., Atkinson, J. D., and Webb, M. E.: Ice nucleation by particles immersed in supercooled cloud droplets, Chem. Soc. Rev., 41, 6519-6554, 10.1039/C2CS35200A, 2012.

Plane, J. M. C., Feng, W., and Dawkins, E. C. M.: The mesosphere and mtals: Chemistry and changes, Chem. Rev., 115, 4497-4541, 10.1021/cr500501m, 2015.

Pruppacher, H. R., and Klett, J. D.: Microphysics of clouds and precipitation, D. Reidel Publishing Company, Dordretch, Holland, 1978.

Salcedo, D., Molina, L. T., and Molina, M. J.: Homogeneous freezing of concentrated aqueous nitric acid solutions at polar stratospheric temperatures, J. Phys. Chem. A, 105, 1433-1439, 10.1021/jp001639s, 2001.

Saunders, R. W., Dhomse, S., Tian, W. S., Chipperfield, M. P., and Plane, J. M. C.: Interactions of meteoric smoke particles with sulfuric acid in the Earth's stratosphere, Atmos. Chem. Phys., 12, 4387-4398, 10.5194/acp-12-4387-2012, 2012.

Schneider, J., Weigel, R., Klimach, T., Dragoneas, A., Appel, O., Hünig, A., Molleker, S., Köllner, F., Clemen, H. C., Eppers, O., Hoppe, P., Hoor, P., Mahnke, C., Krämer, M., Rolf, C., Grooß, J. U., Zahn, A., Obersteiner, F., Ravegnani, F., Ulanovsky, A., Schlager, H., Scheibe, M., Diskin, G. S., DiGangi, J. P., Nowak, J. B., Zöger, M., and Borrmann, S.: Aircraft-based observation of meteoric material in lower-stratospheric aerosol particles between 15 and 68 °N, Atmos. Chem. Phys., 21, 989-1013, 10.5194/acp-21-989-2021, 2021.

Steiner, M., Luo, B., Peter, T., Pitts, M. C., and Stenke, A.: Evaluation of polar stratospheric clouds in the global chemistry–climate model SOCOLv3.1 by comparison with CALIPSO spaceborne lidar measurements, Geosci. Model Dev., 14, 935-959, 10.5194/gmd-14-935-2021, 2021.

Subasinghe, D., Campbell-Brown, M. D., and Stokan, E.: Physical characteristics of faint meteors by light curve and high-resolution observations, and the implications for parent bodies, Mon. Not. Royal Astro. Soc., 457, 1289-1298, 2016.

Taesler, I., Delaplane, R. G., and Olovsson, I.: Hydrogen bond studies. XCIV. Diaquaoxonium ion in nitric acid trihydrate, Acta Cryst. Sec. B, 31, 1489-1492, doi:10.1107/S056774087500550X, 1975.

Tarn, M. D., Sikora, S. N. F., Porter, G. C. E., Shim, J.-u., and Murray, B. J.: Homogeneous freezing of water using microfluidics, Micromachines, 12, 223, 2021.

Taylor, S., Matrajt, G., and Guan, Y.: Fine-grained precursors dominate the micrometeorite flux, Meteorit. Planet. Sci., 47, 550-564, 10.1111/j.1945-5100.2011.01292.x, 2012.

https://doi.org/10.5194/acp-2022-598
Preprint. Discussion started: 29 August 2022

Atmospheric Chemistry and Physics Discussions

Tisdale, R. T., Middlebrook, A. M., Prenni, A. J., and Tolbert, M. A.: Crystallization kinetics of HNO_3/H_2O films representative of polar stratospheric clouds, J. Phys. Chem. A, 101, 2112-2119, 10.1021/jp9624156, 1997.

Tritscher, I., Pitts, M. C., Poole, L. R., Alexander, S. P., Cairo, F., Chipperfield, M. P., Grooß, J.-U., Höpfner, M., Lambert, A., Luo, B., Molleker, S., Orr, A., Salawitch, R., Snels, M., Spang, R., Woiwode, W., and Peter, T.: Polar Stratospheric Clouds: Satellite Observations, Processes, and Role in Ozone Depletion, Rev. Geophys., 59, e2020RG000702, https://doi.org/10.1029/2020RG000702, 2021.

Voigt, C., Schlager, H., Luo, B. P., Dörnbrack, A., Roiger, A., Stock, P., Curtius, J., Vössing, H., Borrmann, S., Davies, S., Konopka, P., Schiller, C., Shur, G., and Peter, T.: Nitric Acid Trihydrate (NAT) formation at low NAT supersaturation in Polar Stratospheric Clouds (PSCs), Atmos. Chem. Phys., 5, 1371-1380, 10.5194/acp-5-1371-2005, 2005.

Wang, Y., and Forssberg, E.: Production of carbonate and silica nano-particles in stirred bead milling, Int. J. Mineral Processing, 81, 1-14, https://doi.org/10.1016/j.minpro.2006.05.007, 2006.

Wegner, T., Grooß, J. U., von Hobe, M., Stroh, F., Sumińska-Ebersoldt, O., Volk, C. M., Hösen, E., Mitev, V., Shur, G., and Müller, R.: Heterogeneous chlorine activation on stratospheric aerosols and clouds in the Arctic polar vortex, Atmos. Chem. Phys., 12, 11095-11106, 10.5194/acp-12-11095-2012, 2012.

Weigel, R., Volk, C. M., Kandler, K., Hösen, E., Günther, G., Vogel, B., Grooß, J. U., Khaykin, S., Belyaev, G. V., and Borrmann, S.: Enhancements of the refractory submicron aerosol fraction in the Arctic polar vortex: feature or exception?, Atmos. Chem. Phys., 14, 12319-12342, 10.5194/acp-14-12319-2014, 2014.

Wex, H., DeMott, P. J., Tobo, Y., Hartmann, S., Rösch, M., Clauss, T., Tomsche, L., Niedermeier, D., and Stratmann, F.: Kaolinite particles as ice nuclei: learning from the use of different kaolinite samples and different coatings, Atmos. Chem. Phys., 14, 5529-5546, 10.5194/acp-14-5529-2014, 2014.

Whale, T. F., Holden, M. A., Wilson, T. W., O'Sullivan, D., and Murray, B. J.: The enhancement and suppression of immersion mode heterogeneous ice-nucleation by solutes, Chem. Sci., 9, 4142-4151, 10.1039/C7SC05421A, 2018.

Wise, M. E., Brooks, S. D., Garland, R. M., Cziczo, D. J., Martin, S. T., and Tolbert, M. A.: Solubility and freezing effects of Fe^{2+} and Mg^{2+} in H_2SO_4 solutions representative of upper tropospheric and lower stratospheric sulfate particles, J. Geophys. Res.: Atmos., 108, 4434, 10.1029/2003JD003420, 2003.

Wood, S. E.: Nucleation and growth of carbon dioxide ice crystals in the Martian atmosphere, University of California, Los Angeles, 1999.